Cell atlas of the Atlantic salmon spleen reveals immune cell heterogeneity and cellspecific responses to bacterial infection

Fish and Shellfish Immunology 145 (2024) 109358

Contents lists available at ScienceDirect

Fish and Shellfish Immunology

journal homepage: www.elsevier.com/locate/fsi

Cell atlas of the Atlantic salmon spleen reveals immune cell heterogeneity and cell-specific responses to bacterial infection

Jianxuan Sun [a], Rose Ruiz Daniels [a], Adam Balic [a,b], Adriana M.S. Andresen [c], Håvard Bjørgen [d], Ross Dobie [e], Neil C. Henderson [e,f], Erling Olaf Koppang [d], Samuel A.M. Martin [g], Johanna Hol Fosse [c], Richard S. Taylor [a], Daniel J. Macqueen [a,*]

[a] The Roslin Institute and Royal (Dick) School of Veterinary Studies, The University of Edinburgh, Midlothian, UK
[b] Department of Biochemistry and Pharmacology, Bio21 Molecular Science and Biotechnology Institute, The University of Melbourne, Parkville, Victoria, Australia
[c] Norwegian Veterinary Institute, Ås, Norway
[d] Unit of Anatomy, Faculty of Veterinary Medicine, Norwegian University of Life Sciences, Ås, Norway
[e] Centre for Inflammation Research, The Queen's Medical Research Institute, Edinburgh BioQuarter, University of Edinburgh, Edinburgh, UK
[f] MRC Human Genetics Unit, Institute of Genetics and Cancer, University of Edinburgh, Edinburgh, UK
[g] Scottish Fish Immunology Research Centre, School of Biological Sciences, University of Aberdeen, Aberdeen, UK

A B S T R A C T

The spleen is a conserved secondary lymphoid organ that emerged in parallel to adaptive immunity in early jawed vertebrates. Recent studies have applied single cell transcriptomics to reveal the cellular composition of spleen in several species, cataloguing diverse immune cell types and subpopulations. In this study, 51,119 spleen nuclei transcriptomes were comprehensively investigated in the commercially important teleost Atlantic salmon (*Salmo salar* L.), contrasting control animals with those challenged with the bacterial pathogen *Aeromonas salmonicida*. We identified clusters of nuclei representing the expected major cell types, namely T cells, B cells, natural killer-like cells, granulocytes, mononuclear phagocytes, endothelial cells, mesenchymal cells, erythrocytes and thrombocytes. We discovered heterogeneity within several immune lineages, providing evidence for resident macrophages and melanomacrophages, infiltrating monocytes, several candidate dendritic cell subpopulations, and B cells at distinct stages of differentiation, including plasma cells and an *igt* + subset. We provide evidence for twelve candidate T cell subsets, including *cd4*+ T helper and regulatory T cells, one *cd8*+ subset, three γδT subsets, and populations double negative for *cd4* and *cd8*. The number of genes showing differential expression during the early stages of *Aeromonas* infection was highly variable across immune cell types, with the largest changes observed in macrophages and infiltrating monocytes, followed by resting mature B cells. Our analysis provides evidence for a local inflammatory response to infection alongside B cell maturation in the spleen, and upregulation of *ccr9* genes in *igt* + B cells, T helper and *cd8*+ cells, and monocytes, consistent with the recruitment of immune cell populations to the gut to deal with *Aeromonas* infection. Overall, this study provides a new cell-resolved perspective of the immune actions of Atlantic salmon spleen, highlighting extensive heterogeneity hidden to bulk transcriptomics. We further provide a large catalogue of cell-specific marker genes that can be leveraged to further explore the function and structural organization of the salmonid immune system.

1. Introduction

The spleen is the only secondary lymphoid organ present in all jawed vertebrates [1]. In mammals, the spleen contains stromal cells, mesenchymal stem cells and various leukocyte populations [2,3] and is split into two discrete compartments. The red pulp consists of red blood cells and macrophages that capture pathogens, recycle iron and remove damaged blood cells, whereas the white pulp is the primary lymphoid compartment where T cells, B cells, and antigen presenting cells (APCs) reside [2,4,5]. The white and red pulp is bridged by the marginal zone, enriched in specific subsets of B cells and macrophages [6]. In mammals and some avian species, germinal centers (GCs) are specialized microstructures within the white pulp that form during infection or immunization [7]. Within GCs, B cells proliferate before undergoing somatic hypermutation and affinity maturation, leading to selection for clonal B cells with high affinity to antigens from the invading pathogen. This process promotes the generation and export of antibody-secreting plasma B cells that are the basis for adaptive humoral immunity, along with memory B cells responsible for long-term immunological memory [7–9]. The molecular and cellular foundations of splenic GCs date back to the jawed vertebrate ancestor [10].

Teleosts lack lymph nodes and Peyer's patches, and the spleen is primarily responsible for immune surveillance of peripheral blood antigens. Teleosts do not develop GCs in their secondary lymphoid organs,

* Corresponding author.
E-mail address: daniel.macqueen@roslin.ed.ac.uk (D.J. Macqueen).

https://doi.org/10.1016/j.fsi.2024.109358
Received 9 November 2023; Received in revised form 23 December 2023; Accepted 2 January 2024
Available online 3 January 2024

and the mechanisms for clonal expansion of B cells in the spleen remain poorly understood. Nevertheless, the gross organization of the teleost spleen seems similar to that of mammals as far as it can be divided into a red and white pulp, the latter containing ellipsoids surrounded by different leukocyte populations [11]. Also, within the spleen, distinct pigmented cells called melanomacrophages reside. In some teleosts, these cells tend to aggregate and form cellular clusters known as melanomacrophage centers (MMCs) [12]. MMCs have been proposed by some authors as functionally analogous to mammalian GCs. For example, a recent study in zebrafish (*Danio rerio*) proposed that MMCs act as structures for B cell selection, with melanomacrophages assuming a role akin to follicular dendritic cells [13]. Despite such work, the hypothesis that MMCs are functionally analogous to mammalian GCs has remained controversial [14]. A recent study of rainbow trout (*Oncorhynchus mykiss*) following parasitic infection indicated that MMCs associated with aggregates of B and T cells including antigen-specific B cells [15]. These MMC-associated lymphoid aggregates were suggested as sites of somatic hypermutation and expressed high levels of activation-induced cytidine deaminase [15].

Recent single cell transcriptomic studies in mammals have revealed heterogeneity within several spleen cell lineages [16–18], deepening our understanding of splenic spatial organisation [19,20]. Single cell transcriptomics is currently being uptaken in non-model teleosts as the gold standard for gene expression profiling, and transforming our understanding of immune cell heterogeneity in a range of species [21,22]. This approach captures the cellular origin of gene expression, allowing different cell types and their subsets to be distinguished under distinct developmental and functional states. Recent single cell transcriptomic studies of the spleen in Atlantic cod (*Gadus morhua*), which belongs to a group of fishes lacking MHC-II genes and $CD4^+$ T cells, identified candidate natural killer-like (NK-like) cells and dendritic cells (DCs) alongside heterogeneity in T and B lymphocytes [23]. Comparable immune cell heterogeneity has been observed in the spleen of turbot (*Scophthalmus maximus*) [24,25], as well as several other fish species [22].

Atlantic salmon (*Salmo salar* L.) is globally among the most important farmed fishes [26,27]. A detailed understanding of immune cell heterogeneity and function is important to help reduce disease outbreaks in salmon aquaculture, by supporting the design of rational approaches to vaccination and selective breeding for disease resistance. Genomic studies of the immune system in Atlantic salmon are complicated by the impact of whole genome duplication (WGD) events in salmonid evolution. This notably includes a salmonid-specific WGD (Ss4R) event, which occurred on top of an earlier teleost-specific third WGD event [28–30]. These WGDs complicate single cell analyses and interpretations, with multiple paralogous genes typically sharing co-orthology to cell marker genes defined in model species [22]. Recent single cell studies in Atlantic salmon have identified immune cell heterogeneity within the liver [31], gill [32] and head kidney [33]. Single cell transcriptomic studies in rainbow trout have also provided insight into the heterogeneity of circulating B cells [34]. However, no single cell transcriptomic studies of the salmonid spleen have been conducted so far, including during the course of an infection.

The primary aim of this study was to investigate cellular heterogeneity within the spleen of Atlantic salmon during the early response to bacterial infection. Using single nuclei RNA-seq (snRNA-seq), we report a comprehensive atlas of spleen cells, revealing heterogeneity within several immune cell lineages, before exploring cell-resolved responses to *Aeromonas salmonicida*, an ongoing cause of disease outbreaks in salmonid aquaculture [35]. Our findings enhance knowledge of the salmonid spleen and immune response, and provide an extensive catalogue of cell-specific marker genes that can be leveraged to support the development of disease control efforts built on a foundation of understanding the cellular basis for immunity.

2. Materials and methods

2.1. Samples and snRNA-Seq data generation

Spleen samples were taken during an experiment described elsewhere [31]. The animal work was carried out in compliance with the UK Animals (Scientific Procedures) Act 1986 under Home Office license PFF8CC5BE and approved by the ethics committee of the University of Aberdeen. Twenty fish representing sexually immature freshwater parr (mean/s.d. fork length: 12.7 cm/0.6 cm; approximately 8 months in age) were anaesthetized using 2-phenoxyethanol (2.5 mL in 10L water/0.0025 % v/v) and administered an intraperitoneal injection of either PBS (0.5 mL) (n = 10 control fish) or the pathogenic Hooke strain of *Aeromonas salmonicida* (2×10^5 colony forming units/mL in PBS; 0.5 mL/fish) (n = 10 *Aeromonas* infected fish). Samples from all twenty fish were taken 24-h post-injection, after the fish were killed using a Schedule 1 method by destruction of the brain following overdose with 2-phenoxyethanol (0.1 % v/v). A panel of tissue biopsies for spleen, head kidney, gill, blood and liver was sampled from all twenty animals and flash frozen on dry ice before storage at −80 °C. Two control and two *Aeromonas* infected fish were selected on the basis of the expression of pro-inflammatory and acute phase marker genes (reported in Ref. [31]). Our past snRNA-Seq analysis in liver also confirmed an acute phase and inflammatory response was occurring in the *Aeromonas* infected fish [31]. The PBS-injected controls used for snRNA-Seq in this study (n = 2, fork length: 12.5 and 12.8 cm) were from the same fish reported in our previous study [31]. The head kidney samples from these two animals were also used in an snRNA-Seq study reported in the same special issue of this journal [33]. The two control samples used for snRNA-Seq here (n = 2, fork length: 11.7 and 12.5 cm) were from the same animals used in our past liver study [31].

Nuclear isolation followed a method described elsewhere [36] except for an additional filtration step with a 20 μm cell strainer before the cell counting and library preparation steps. The snRNA-Seq libraries were generated using the 10X Genomics Chromium platform, which were sequenced on a NovaSeq 6000 by Novogene UK Ltd generating 2 × 150bp paired end reads.

2.2. Generation of the count matrix

The raw sequence data was checked with FastQC v0.11.9 [37]. Reads were aligned to the unmasked Ssal_v3.1 Atlantic salmon genome (GCA_905237065.2 [38]; downloaded from the Ensembl Genome Browser release 106 (https://www.ensembl.org/Salmo_salar/Info/Index) using StarSolo v2.7.8a [39], which was also used to attribute reads to cellular barcodes and de-duplicate unique molecular identifiers (UMIs). The analysis was restricted to protein coding genes by specifying annotations with a gene_biotype of "protein coding". The genome index was generated with standard settings and "sjdbOverhang" set to 149 to account for the 150bp read length. Parameters "outFilterScoreMinOverLread" and "outFilterMatchNminOverLread" were set to 0.4 to maximise mapping length and the proportion of uniquely mapped reads. Reads were mapped with the "STAR" command and following settings: soloCBstart = 1, soloCBlen = 16, soloUMIstart = 17, soloUMIlen = 12, soloBarcodeReadLength = 0, soloUMIfiltering = MultiGeneUMI_CR, soloCellFilter = EmptyDrops_CR, outFilterMatchNmin = 66, outFilterScoreMin = 30, outFilterMatchNminOverLread = 0.4, outFilterScoreMinOverLread = 0.4, soloMultiMappers = EM, limitOutSJcollapsed = 2,000,000, soloCellReadStats = Standard. Detailed mapping statistics for each sample are provided in Supplementary Table 1.

2.3. Filtering and quality control

Filtering was first conducted in Starsolo, where UMIs and gene counts of nuclei were ranked and the lower "elbow point" identified to

remove cellular barcodes with lower UMI or gene counts as likely empty droplets. Further quality control was conducted on each sample using Seurat v4.0.6 [40]. Background RNA contamination was estimated and removed using SoupX [41]. Next, individual nuclei with UMIs <300 or gene counts <200, and/or showing mitochondria and ribosome genes >10 % were removed. The "SCTransform" function was used to normalize the data, followed by centring, scaling, principal component analysis (PCA) and an initial high resolution clustering (performed with 20 principal components and resolution of '2' in the "FindClusters" Seurat command) to identify additional clusters of empty droplets [42]. Populations that lacked distinguishing markers (see section, 'Differential gene expression tests') were removed as likely empty droplets or poor quality nuclei. Doublets were also identified and removed using the R package ScDblFinder v1.10.0 [43]. A manual quality control step was performed to remove further potential doublets once cell identity was established (described in section 'Assignment of cellular identity').

2.4. Assignment of cellular identity

The four samples were merged into one Seurat object using the "merge" function. Harmony v0.1.0 [44] was then used to reduce confounding sample-specific batch effects. Each cluster was assigned to a major cell lineage using *a priori* defined marker genes (Supplementary Table 2). Gene annotations were taken from the Ensembl Genome Browser annotation for Atlantic salmon (Ssal_v3.1). For genes lacking annotations, the name of the nearest Ensembl annotated orthologue in rainbow trout (USDA_OmykA_1.1), zebrafish (*Danio rerio* – GRCz11) or mouse (*Mus musculus*– GRCm39) was adopted (Supplementary Table 3) using the R package BiomaRt v2.52.0 [45]. Cell populations that expressed *a priori* defined markers (Supplementary Table 2) or lineage-distinguishing markers (Supplementary Table 4; see section 'Differential gene expression tests') of distinct cell lineages, but lacked any unique distinguishing markers in the differential gene expression (DGE) test, were eliminated as doublets. Detailed statistics including the number and proportion of each cell lineage for each sample are provided in Supplementary Table 5. Populations identified as erythrocytes and thrombocytes were removed from the analysis at this point.

For the additional cell lineage specific analysis, all major populations were split into separate Seurat objects and additional clustering was done using default parameters (resolution = 0.8). Each subpopulation was then assigned an identity based on canonical marker genes from the literature (Supplementary Table 6). This approach of extracting and re-clustering cell lineages of interest was chosen over high-resolution global clustering to reveal more biologically meaningful heterogeneity [22].

2.5. Differential gene expression tests

To identify gene expression profiles and marker genes for different cell populations, a DGE test was performed using the Seurat "FindAllMarkers" function [40] based on the Wilcoxon rank sum test. This approach involves comparing the expression of each gene in a specific cell population with its expression in all other cells (results in Supplementary Table 4). Genes with Bonferroni-adjusted $p < 0.05$ and average log2FC > 0.40 were considered as significantly differentially expressed. Genes significantly upregulated in each population were considered markers. For the cell lineage-specific DGE analysis, the background was set as all nuclei analysed for the major cell lineage being examined (Supplementary Tables 7–13). We also provide summary statistics about the identified cell populations across all four biological samples (Supplementary Table 14).

To examine the cell-specific response to *Aeromonas*, we performed DGE tests within the same cell clusters and subpopulations, contrasting the control and *Aeromonas* infected fish using the "FindMarkers" function in Seurat (Supplementary Tables 15–16). This was done for the eight major cell lineages defined by global clustering (Supplementary Table 15), and for immune cell subpopulations defined by cell lineage specific clustering (Supplementary Table 16). Genes with FDR adjusted $p < 0.05$ were considered differentially expressed.

2.6. Correlation and GO enrichment analyses

To explore the transcriptome-wide correlation between subpopulations of mononuclear phagocytes (MPs) and the MP-like *csf1r*-cells (see section 3.2.4), we conducted a correlation analysis after subclustering MPs alongside the MP-like *csf1r*-cells. The subclustering was done as described above. The correlation analysis employed the "cor" function from the R package stats v4.3.1 [46] and was performed using the estimated expression levels of all expressed genes for pairwise combinations across all the identified MP subpopulations, including the MP-like *csf1r*-cluster.

To further investigate the phenotype of MP subpopulations including the MP-like *csf1r*-cluster, we conducted Gene Ontology-Biological Process (GO-BP) enrichment analyses using the R package clusterProfiler v4.8.3 [47] (Supplementary Table 17). These analyses were performed individually for each identified MP subpopulation, employing all significant marker genes (adjusted $p < 0.05$) as the input (Supplementary Table 10), with the background gene set representing all genes expressed across the MP lineage (including the MP-like *csf1r*-cluster).

3. Results and discussion

3.1. Major cell populations in the atlantic salmon spleen

Following filtering and quality control steps, we used snRNA-Seq to profile 51,119 single nuclei transcriptomes across the four Atlantic salmon spleen samples, with a median of 1648 genes (s.d. 971) captured per nuclei. Our recent work has shown that snRNA-Seq provides an excellent representation of cellular diversity in salmonid tissues, and has advantages compared to widely used scRNA-Seq methods [22,33]. Eight major cell lineages were identified using unbiased graph-based clustering [48], with cell identity initially assigned using pre-defined marker genes (Fig. 1A and B; markers in Supplementary Table 2) supported by examining marker genes defined by DGE tests across the distinct clusters (Fig. 1C; Supplementary Table 4). In the text that follows, we provide Ensembl identifiers for all mentioned genes, inclusive of any identified paralogues for a particular cell cluster.

B cells were identified using *ebf1* (ENSSSAG00000079780, ENSSSAG00000070298) [49], *cd79a* (ENSSSAG00000113980) [50], *tcf7l2* (ENSSSAG00000066753) [51], *vav2* (ENSSSAG00000009589) [52] and *swap70* (ENSSSAG00000115076, ENSSSAG00000118232) [53] as marker genes. T cells were identified using *cd3e* (ENSSSAG00000076824) [54], *tcf7* (ENSSSAG00000006857, ENSSSAG00000064204) [55], *bcl11b* (ENSSSAG00000071984, ENSSSAG00000045088) [56], *tox2* (ENSSSAG00000113443) and *tbx21* (ENSSSAG00000015324) as markers. Natural killer (NK)-like (NK-L) cells were annotated using *runx3* (ENSSSAG00000064246) [57], *zeb2b* (ENSSSAG00000050763) [58], *prf1.3* (ENSSSAG00000002801, ENSSSAG00000009129), *aqp1* (ENSSSAG00000117352) and *mafa* (ENSSSAG00000108168/ENSSSAG00000052644) genes, which were also markers for NK-L clusters described in Atlantic salmon liver [31]. Mononuclear phagocytes (MPs) were identified using *cd74* (ENSSSAG00000091373, ENSSSAG00000004635, ENSSSAG00000062736) [59], *csf1r* (ENSSSAG00000061479, ENSSSAG00000001705) [60], *mpeg1* (ENSSSAG00000076214) [35] and *nrxn1* (ENSSSAG00000057796) [61]. Granulocytes were marked by high expression of *mmp9* (ENSSSAG00000069874) [62], *mmp13* (ENSSSAG00000070495) [63], *lect2* (ENSSSAG00000115953) [64] and *csf3r* (ENSSSAG00000041566) [65]. Endothelial cells were identified by their high expression of *egfl7* (ENSSSAG00000083641) [66] and *kdrl* (ENSSSAG00000046825) [67], and mesenchymal cells were identified using *hmcn1* (ENSSSAG00000066417) [68] and *tpm1*

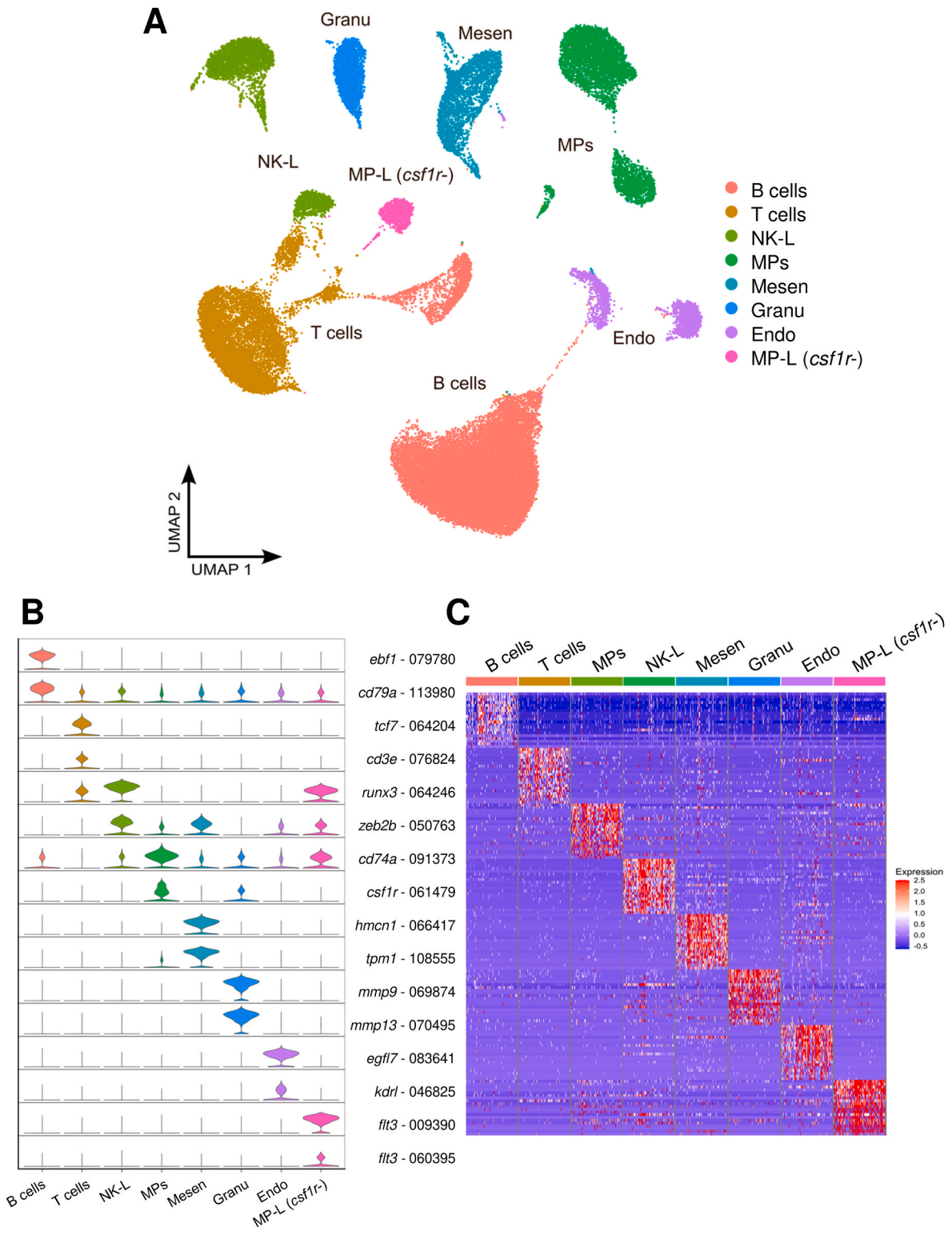

Fig. 1. Cell populations identified in the Atlantic salmon spleen. **A.** UMAP visualisation of eight major spleen cell types. **B.** Violin plots demonstrating the expression of marker genes. **C.** Heatmap of the top 20 differentially expressed genes for each cell cluster. Columns represent cells; rows represent genes. Endo: endothelial cells, Granu: granulocytes, Mesen: mesenchymal cells, MPs: mononuclear phagocytes, and NK-L: natural killer-like cells. The unique ending of Ensembl gene identifiers is provided for all genes shown.

(ENSSSAG00000108555) [69] as markers.

Using the above markers, 7 major cell populations were identified, with the following proportions of all nuclei: B cells (46.8 %), T cells (16.7 %), MPs (11.0 %), NK-L cells (8.0 %), mesenchymal cells (6.6 %), granulocytes (4.6 %), and endothelial cells (4.4 %). We also identified a distinct cluster that comprised ~2 % of all nuclei and had many distinct marker genes, most strikingly two paralogues of *flt3* (ENSSSAG00000009390/ENSSSAG00000060395) (Fig. 1B; Supplementary Table 4), but could not easily be assigned to any of the major leukocyte lineages. This population shared markers genes with multiple other

clusters from the myeloid and lymphoid lineages, including *atp11c* (NK-L) (ENSSSAG00000055816), *tox2* (T cells) (ENSSSAG00000080613/ ENSSSAG00000074925), *vav3* (granulocytes) (ENSSSAG00000067657), *and sftpba* (B cells) (ENSSSAG00000049747) (Supplementary Table 4). *flt3* is a classic marker of DCs [70], raising the hypothesis that this population represents a DC, which should therefore have clustered within the MPs. However, this population did not express all the marker genes used to define the MP lineage, lacking expression of the *cfsr1* paralogues mentioned above, though it did express *mpeg1* (despite not being a significant marker gene) to a level higher than all cell types barring MPs, and also shared two *cd74* paralogues (ENSSSAG00000062736 and ENSSSAG00000004635) as markers in common with MPs (e.g. Fig. 1B), strongly indicating an APC. At this stage, we named this cluster as *csf1r*- MP-like cells ('MP-L *csf1r*-') (Supplementary Table 4) and report on its characteristics in relation to heterogeneity observed within the broader MP lineage in a later section (Section 3.2.4).

All four samples contributed a significant proportion of sequenced nuclei to each of the identified major cell populations, with no major differences observed in contribution of the nuclei derived from the control and infected samples (Supplementary Fig. 1).

Cell lineage-specific analyses revealed differences in heterogeneity across the major spleen cell types. Several immune lineages exhibited marked heterogeneity within the identified clusters (explored in the following sections). While six granulocyte clusters were identified, each had few specific marker genes, making it challenging to understand the biological relevance of this heterogeneity (Supplementary Fig. 2; Supplementary Table 11). Likewise, we identified a very limited number of specific markers for four identified mesenchymal cell clusters (Supplementary Fig. 3; Supplementary Table 12).

The endothelial cells formed two clusters interpreted to represent arterial microvascular and capillary-venous sinusoidal endothelial cells (including the population sometimes referred to as littoral cells [71]), respectively (Supplementary Fig. 4). The arterial microvascular cluster was enriched for the arterial markers *mecom* (ENSSSAG00000041461) [72], angiogenic markers including *dll4* (ENSSSAG00000001347) [73] and *flt1* (ENSSSAG00000065213) [74], and general vascular markers such as *pecam1a* (ENSSSAG00000003562) [75] and *robo4* (ENSSSAG00000051277) [76]. In contrast, markers of the capillary-venous sinusoidal endothelial cluster included the vascular marker *egfl7* (ENSSSAG00000083641) [77], the venous marker *plvapb* (ENSSSAG00000040305) [78,79], and the littoral cell marker *fhod1* (ENSSSAG00000058596) [71]. This cluster showed a profile consistent with a scavenging and activated phenotype, with similarities to the major capillary population observed in Atlantic salmon head kidney [33]. Scavenger-associated markers included *stab1* (ENSSSAG00000067902) [75] and *mrc1* (ENSSSAG00000073565) [80]. Moreover, several marker genes have known roles in leukocyte guidance, including *vcam1b* (ENSSSAG00000043624) [81], *cxcl12* (ENSSSAG00000117767) [82] and *ccl19b* (ENSSSAG00000002773) [83] (Supplementary Fig. 4; Supplementary Table 13).

3.2. Heterogeneity in several immune cell lineages

We clustered the immune cell lineages to the exclusion of other cell types, and annotated subpopulations based on marker genes identified in the literature. DGE tests for each subpopulation (Supplementary Tables 7–10) were performed against the background of other cells in the same lineage. Heterogeneity was captured in B cells (21,652 nuclei, representing four clusters named B1 to B4) (Fig. 2), T cells (7173 nuclei, representing twelve clusters named T1 to T12) (Fig. 3), NK-like cells (3422 nuclei, representing three clusters named NK-L1 to NK-L3) (Supplementary Fig. 5) and MPs (5652 nuclei, representing eight clusters named MP1 to MP7, plus MP-L *csf1r*-) (Figs. 4 and 5).

3.2.1. Distinct B cell subpopulations in the Atlantic salmon spleen

We identified four B cell subpopulations (B1 to B4) (Fig. 2A and B; marker genes provided in Supplementary Table 7) (Fig. 2C; Supplementary Table 14). We analysed these subpopulations from two perspectives: immunoglobulin gene expression and differentiation status. We first examined the expression of the three teleost immunoglobulin isotypes *igm* (ENSSSAG00000004118 and ENSSSAG00000048830), *igd* (ENSSSAG00000105128), and *igt* (ENSSSAG00000101183, ENSSSAG00000109113 and ENSSSAG00000115151) (Fig. 2D). To further classify the B cell developmental status subsets, we used genes encoding the transcription factors *ebf1* (ENSSSAG00000079780, ENSSSAG00000070298 and ENSSSAG00000041858) [84], *xbp1* (ENSSSAG00000071607, ENSSSAG00000093856) [85], *pax5* (ENSSSAG00000104911) [86] and *blimp1/prdm1* (ENSSSAG00000062775) [87,88].

B1 and B2 appeared to represent resting mature B cells, with both showing potential differences in proportion between control and infected samples (Fig. 2C; see section 3.3.1). B1, the most abundant subset (17,664 nuclei, 81.6 % of B cells), was characterized by high expression of *prkcba* (ENSSSAG00000094876, ENSSSAG00000085436) [89], *negaly6* (ENSSSAG00000015620) [90], *tlr2* (ENSSSAG00000003781) [91], and *cd9b* (ENSSSAG00000097341) (Fig. 2E). A similar B cell population was recently detected in Atlantic salmon head kidney control samples [33]. Considering its rapid response to bacterial infection (described in section 3.3.1), it is possible that B1 represents a B cell subset with innate-like properties, such as marginal zone B cells [6], which in mice are marked by high levels of CD9 [92]. B2 (2194 nuclei, 10.1 % of B cells) was distinguished by enriched expression of *igt* (ENSSSAG00000115151), *cd74b* (ENSSAG00000062736), *tspan18* (ENSSSAG00000041529), *slc7a2* (ENSSSAG00000067111) and *il31ra* (ENSSSAG00000072245). While these genes are associated with immunity in mammals [93–95], their roles in teleosts are not well understood, which limits a more specific annotation for B2 than *igt* + B cells. Again, a similar population was observed in the Atlantic salmon head kidney [33].

B3 and B4 (comprising 1332 and 462 nuclei, 6.2 and 2.1 % of B cells, respectively) were characterised by increased expression of the canonical plasmablast/plasma cell markers *cr3l2* (ENSSSAG00000055328) [96], *ppib* (ENSSSAG00000064063) [23], *irf4b* (ENSSSAG00000009083) [97] and a series of immunoglobulin coding genes (*ighv6-1*; ENSSSAG00000004118), *igkv4-1*; ENSSSAG00000101162 and *igl3v5*; ENSSSAG00000042037) (Fig. 2E). As B cells develop towards plasma cells, *ebf1* and *pax5* expression decreases, while *xbp1* and *blimp1/prdm1* expression increases [98]. Compared to B4, lower expression of *pax5* and *igm* and higher expression of *xbp1* and *blimp1/prdm1* indicate that B3 represents mature plasma cells [98] (Fig. 2E). B4 most likely represents plasmacytes, with increased expression of endoplasmic reticulum genes (*hsp90b1*; ENSSSAG00000043708 and *rps6kb1a*; ENSSSAG00000076220) [99,100] and the proliferation-related genes *prim2* (ENSSSAG00000001875) [101], *pola1* (ENSSSAG00000078390) [102], *mki67* (ENSSSAG00000066170) [103], *cenpe* (ENSSSAG00000073454) [104], *anln* (ENSSSAG00000007105) [105], *ncapd3* (ENSSSAG00000044788) [106] and *top2a* (ENSSSAG00000066721) [107].

3.2.2. Extensive T cell heterogeneity in the Atlantic salmon spleen

Based on the composition of TCR chains, *cd3*+ T lymphocytes in teleost fish can be classified into αβ and γδ T cells [108]. Most studies in Atlantic salmon have focussed on αβT cells, which can be further classified by the presence of the surface glycoproteins CD4 and CD8 (i.e. as $CD4^+$ or $CD8^+$ T cells) [109]. On the other hand, γδT cells have only been functionally characterized at depth in zebrafish, where they make up a higher proportion of T cells than in mammals [108]. Nonetheless, the Atlantic salmon genome retains functional gamma and delta T-cell receptor genes [110].

In this study, we classified T cells based on the expression of CD3

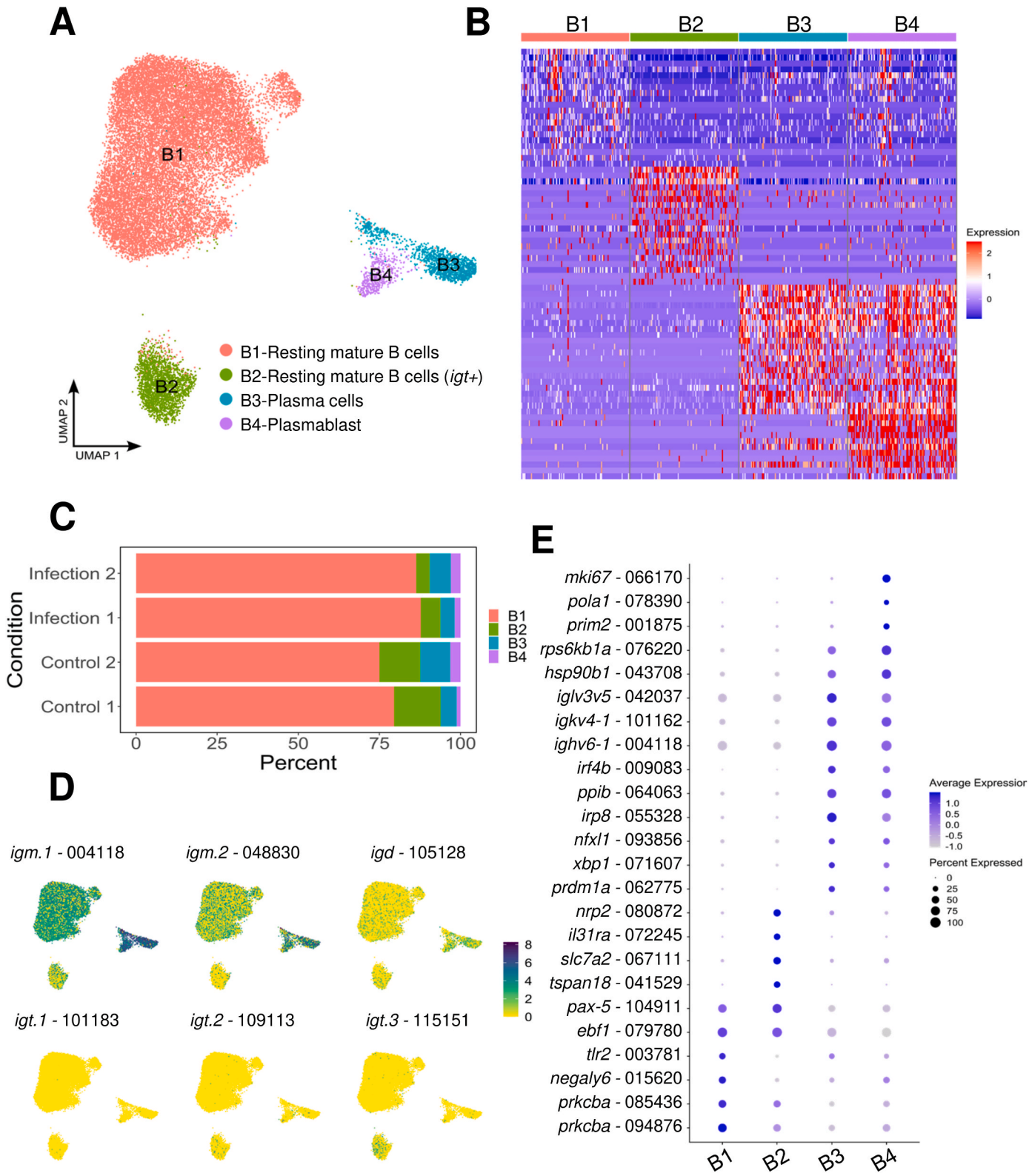

Fig. 2. Identification of B cell subpopulations. **A.** UMAP visualisation of four B cell subpopulations. **B.** Heatmap of top 20 differentially expressed genes for each cluster. Columns and rows represent cells and genes, respectively. **C.** Fraction of each B subpopulation across four biological replicates, including control and *Aeromonas* infection samples. **D.** Feature plots demonstrating the expression of immunoglobulin genes. **E.** Dot plot demonstrating the expression of B cell subpopulation marker genes. The unique ending of Ensembl gene identifiers is provided for all genes shown.

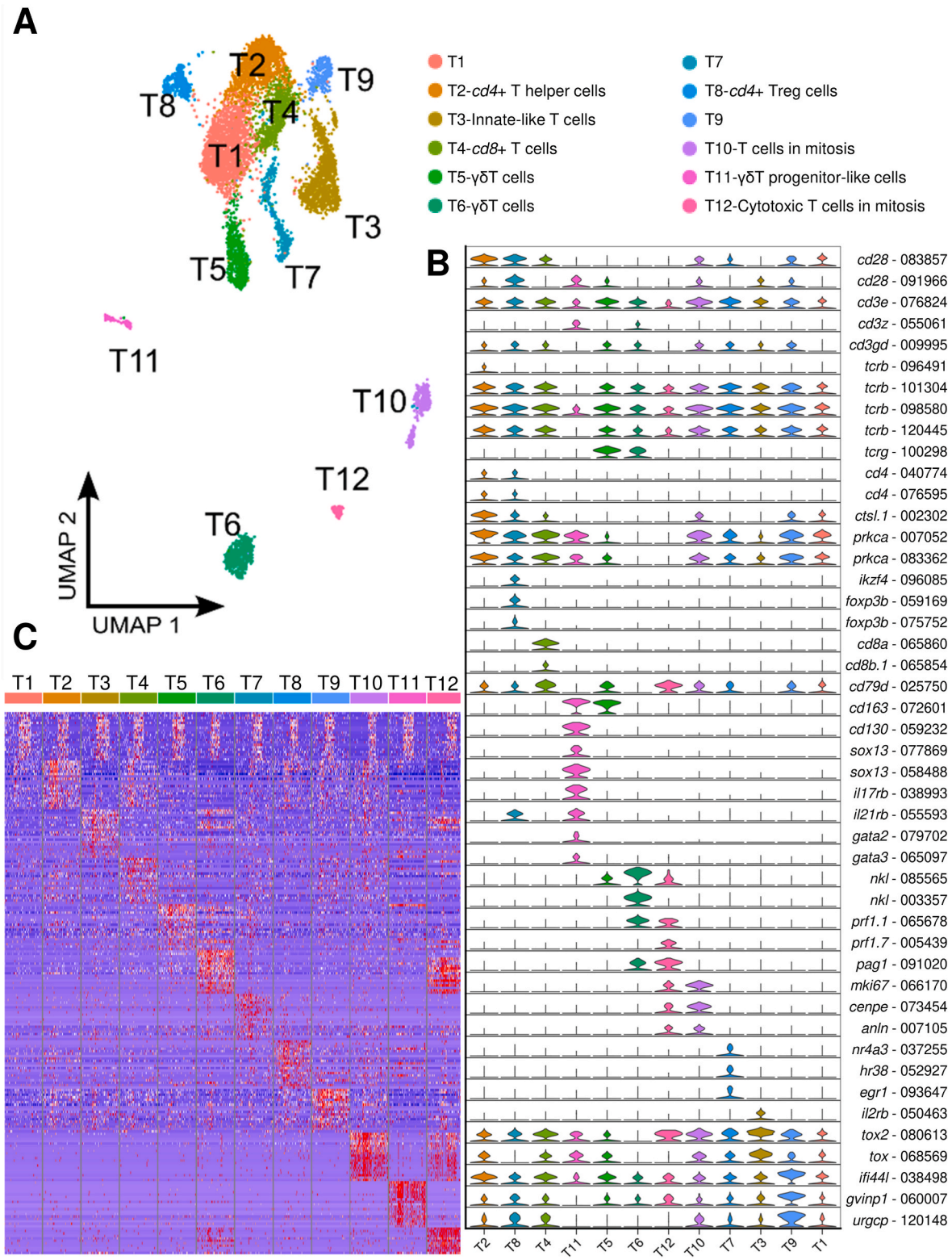

Fig. 3. Identification of T cell subpopulations. **A.** UMAP visualisation of twelve T cell subpopulations. **B.** Violin plots demonstrating the expression of T cell markers and notable cluster enriched genes. **C.** Heatmap of top 20 differentially expressed genes for each cell cluster. Columns represent cells; rows represent genes. The unique ending of Ensembl gene identifiers is provided for all genes shown.

protein complex coding genes (*cd3e*: ENSSSAG00000076824; *cd3z*: ENSSSAG00000055061 and *cd3gd*: ENSSSAG00000009995), T cell receptor (TCR) genes (*tcra*: ENSSSAG00000054449; *tcrb*: ENSSSAG00000096491, ENSSSAG00000101304, ENSSSAG00000098580, ENSSSAG00000120445 and *tcrg*: ENSSSAG00000100298), *cd4* genes (ENSSSAG00000040774, ENSSSAG00000076595, ENSSSAG00000076631, ENSSSAG00000040842), *cd8* genes (*cd8α*: ENSSSAG00000065860; *cd8b.1*: ENSSSAG00000065854 and *cd8b.2*: ENSSSAG00000045680), and *cd28* (ENSSSAG00000083857, ENSSSAG00000091966), a molecule involved in the activation, differentiation and function of T

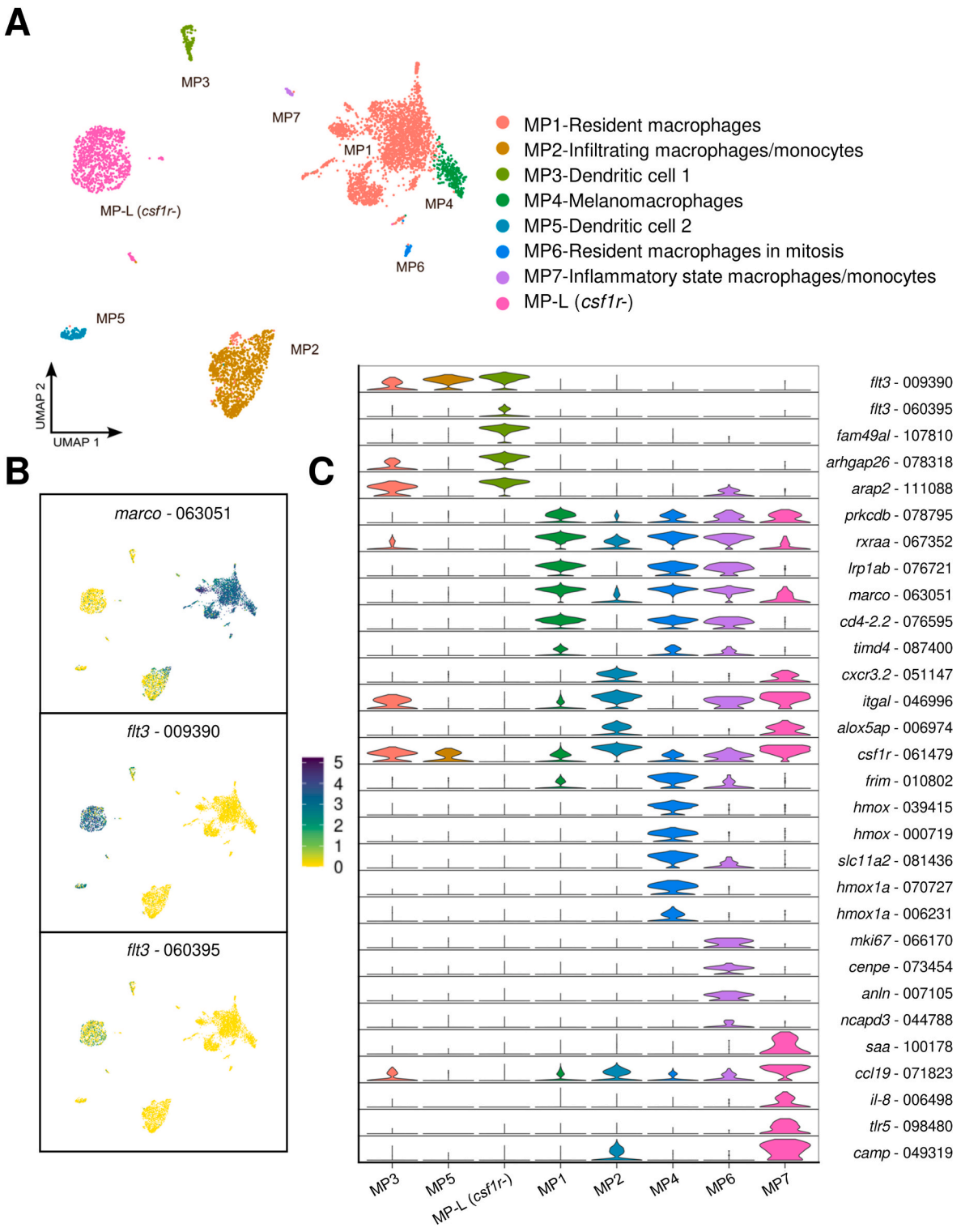

Fig. 4. MP subpopulations **A.** UMAP visualisation of MP subpopulations including MP-L (*csf1r-*). **B.** Feature plots of marker genes distinguishing macrophages/monocytes from DC-like cells. **C.** Violin plot demonstrating the expression of *flt3* in MP-L (*csf1r-*) and macrophage/monocyte subpopulation marker genes. The unique ending of Ensembl gene identifiers is provided for all genes shown.

cells [111].

Twelve T cell clusters named T1 to T12 were identified (Fig. 3). Expression of *tcra* was not detected in any T cell cluster, whereas three out of the four *tcrb* genes were expressed by most subpopulations (Fig. 3C). With the exception of T2 (1135 nuclei, 15.8 % of T cells), T4 (607 nuclei, 8.5 % of T cells) and T8 (334 nuclei, 4.7 % of T cells), all other T cells subpopulations were double negative for *cd4* and *cd8* (Supplementary Table 8). Previous studies in rainbow trout head kidney characterized two types of *cd4*+ T cells, *cd4-1/cd4-2* double-positive and *cd4-2* single-positive [112]. In our data, we found two clusters with enrichment for both *cd4-1* and *cd4-2,* T2 and T8, of which 9.5 % of cells in the clusters were double-positive cell for the two markers. No *cd4-2* single-positive cluster was identified (Fig. 3C). T2 are presumed to represent T helper cells, displaying high expression of molecules

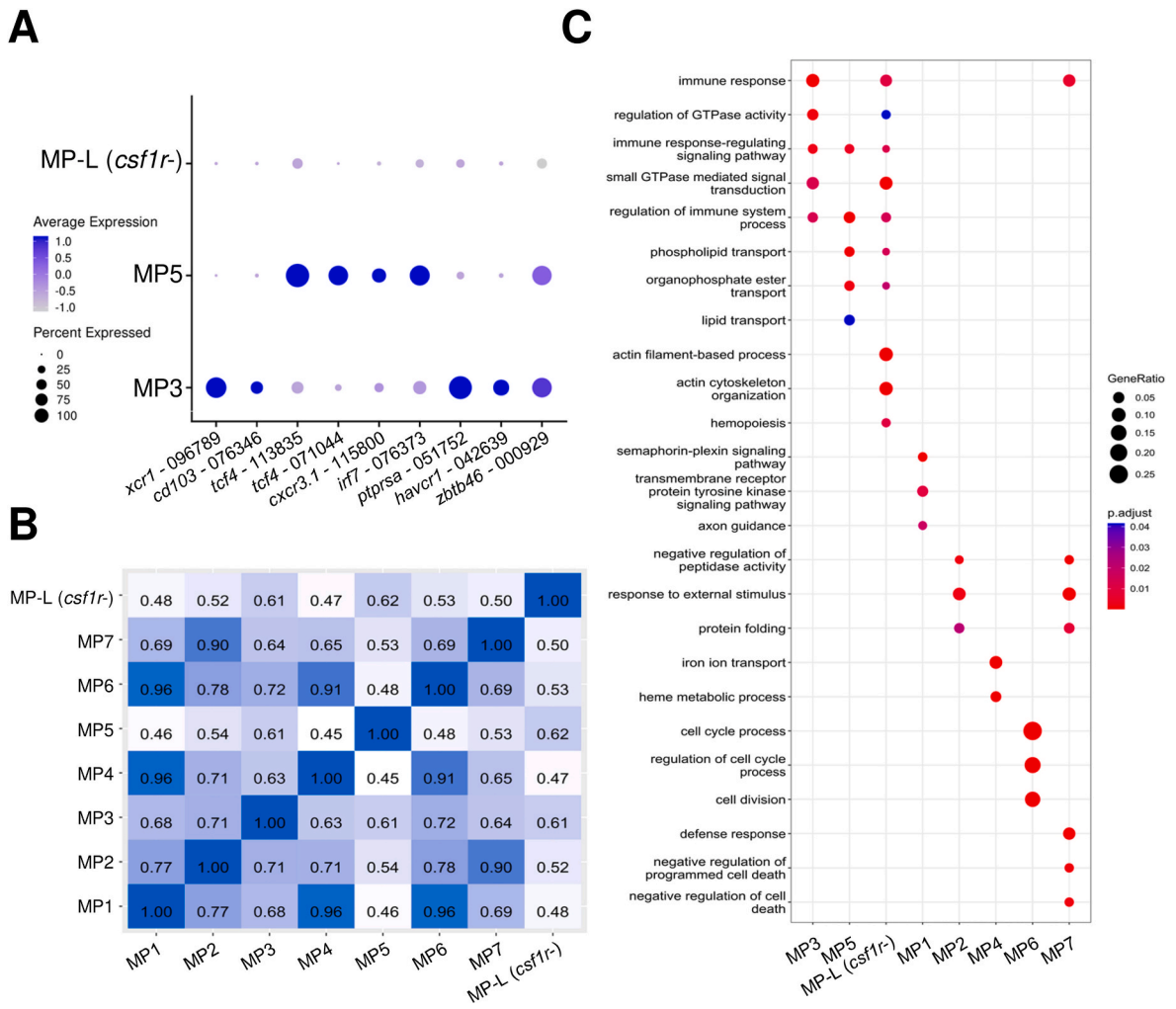

Fig. 5. Relationship of MP-L (*csf1r*-) with other MP subpopulations. **A.** Dot plot showing expression of markers for cDCs and pDCs. **B.** Pairwise correlation of all expressed genes among each MPs subpopulation. **C.** Top GO-BP terms for MP subpopulations enriched among unique marker genes. Gene ratio represents the proportion of genes in the input lists associated with the given GO term.

associated with T cell receptor recycling and the activation of naïve T cells, namely *ctsl* (ENSSSAG00000002302) [113], *prkca* (ENSSSAG00000007052, ENSSSAG00000083362) [114], and *cd28* [115]. T8 showed defining features of regulatory T cells (Tregs), including specific expression of *ikzf4* (ENSSSAG00000096085) [116] and *foxp3b* (ENSSSAG00000059169, ENSSSAG00000075752) [117,118], in addition to *cd4* [119]. Similar *cd4*+ T cell populations were identified in Atlantic salmon head kidney [33].

In the single *cd8*+ T4 subpopulation, we observed increased expression of *cd49d* (alias: *itga4*) (ENSSSAG00000025750), a marker for tissue resident memory T cells in mammals [120,121]. T4 also specifically upregulated *dlg1* (ENSSSAG00000040993), a gene required for the differentiation of memory T cells in mouse [121] (Supplementary Table 8). These cells appeared to differ from *cd8*+ T cells previously isolated from salmonid spleen, which expressed high levels of cytotoxic components perforin, granulysin, and IFN-γ [122], hinting that they could be a type of memory T cell. However, we did not detect expression of Atlantic salmon orthologues of several other memory T cell marker genes in this subpopulation, namely *cd122, cxcr3, cd44 and cd11a* [123]. A single *cd8*+ T cell cluster was also identified in control Atlantic salmon head kidney samples [33], albeit with several cytotoxic genes included as markers.

The specific expression of *tcrg* leads us to propose that T5 (550 nuclei, 7.7 % of T cells) and T6 (491 nuclei, 6.8 % of T cells) are γδT subpopulations. T5 show high expression of a gene annotated *dmbt1* (also known as *cd163*) (ENSSSAG00000072601), a mammalian γδT cell marker [124], while T6 expressed cytotoxic components including granulysin (*nkl*, ENSSSAG00000085565 and ENSSSAG00000003357) and perforin encoding *prf1* genes (ENSSSAG00000065678 and ENSSSAG00000005439), highly expressed in human γδT cells [125]. Very similar T cell subsets to T5 and T6 were identified in Atlantic salmon head kidney control samples [33]. T11 (138 nuclei, 1.9 % of T cells), while lacking *tcrg* expression, showed enrichment of other canonical mammalian γδT cell markers, including *cd163* (ENSSSAG00000072601), *cd130* (ENSSSAG00000059232), *sox13* (ENSSSAG00000077869 and ENSSSAG00000058488), *il17rb* (ENSSSAG00000038993), and *il21rb* (ENSSSAG00000055593) [126]. Studies in mice have shown that *sox13* drives a γδ-lineage differentiation program in developing T cells [127]. These observations suggest T11 may represent prothymic γδT cell progenitors. The high expression of *gata2* (ENSSSAG00000079702, ENSSSAG00000068560) and *gata3* (ENSSSAG00000044928, ENSSSAG00000065097) in T11 aligns with this suggestion [128,129], and a similar T cell subset to T11 was observed in Atlantic salmon head kidney. However, if this is the case, it is not clear why the cells are also present in spleen, unless circulating to reach the thymus. Notably, similar cells were also detected in Atlantic cod spleen [23].

T7 (363 nuclei, 5.1 % of T cells) showed specific expression of transcriptional targets of TCR signalling including *nr4a3* (ENSSSAG00000037255) [130] and *egr1* (ENSSSAG00000093647) [120],

which are rapidly and transiently expressed following T cell activation in mammals. T10 (357 nuclei, 5.0 % of T cells) and T12 (96 nuclei, 1.3 % of T cells) were annotated as proliferating T cells and proliferating cytotoxic T cells, respectively, based on the increased expression of proliferation marker genes, with multiple cytotoxic genes upregulated in T12, several shared otherwise only by T6, although T12 lacked γδT markers. While a similar subset to T10 was observed in the Atlantic salmon head kidney [33], no head kidney T cell subset clearly resembled the profiles of T7 or T12.

T9 (272 nuclei, 3.8 % of T cells) showed upregulation of genes associated with interferon signalling, including *stat1* (ENSSSAG00000093277), *irf1* (encoding interferon regulatory factor 1) (ENSSSAG00000058121), *ifi44* (encoding interferon induced protein 44) (ENSSSAG00000038498 and ENSSSAG00000107768) and the interferon stimulated gene *tapbp* (ENSSSAG00000077407). A similar signature was characterized in a rare human T cell subpopulation termed "IFN signaling–associated gene high T" defined by scRNA-Seq [131]. No subset with a similar profile was identified in the Atlantic salmon head kidney [33]. T3 (1051 nuclei, 14.7 % of T cells) showed some similarity with a double negative innate-like T cell subset observed in Atlantic salmon head kidney [33], with high levels of *il2rb* (also known as *cd122*) (ENSSSAG00000050463), *tox2* (ENSSSAG00000080613), *tox* (ENSSSAG00000068569), and *fcergl* (ENSSSAG00000092386).

The identity of the large T1 subpopulation (1779 nuclei, 24.8 % of T cells) remained elusive, although a similar population that was likewise poorly defined resided in Atlantic salmon head kidney [33]. This cluster, despite expressing T cell marker genes, showed low levels of *cd4* and *cd8* expression, and generally lacked specific marker genes compared to other T cell subsets (Fig. 3B; Supplementary Table 8).

3.2.3. Three NK-L subpopulations

Teleost nonspecific cytotoxic cells (NCCs) and NK-L cells have been described as homologous to mammalian NK cells [132]. While NCCs have been characterized in channel catfish (*Ictalurus punctatus*) and are recognized by the expression of *nccrp1* [133], we lack a comprehensive understanding of the function and surface membrane phenotype of teleost NK-like cells. As *nccrp1* (ENSSSAG00000075920) was not expressed in the cluster presenting marker genes indicative of the NK lineage, we named it NK-L cells (Supplementary Fig. 5). Orthologues of the mammalian NK cell markers *pik3r3b* (ENSSSAG00000079094) [134] and *zeb2b* (ENSSSAG00000050763) [135] were expressed primarily in NK-L1 (2062 nuclei, 60.3 % of NK-like cells) and NK-L3 (298 nuclei, 8.7 % of NK-like cells) (Supplementary Fig. 5). NK-L3 further upregulated proliferation associated marker genes (Supplementary Fig. 5).

Unlike the other two NK-like cell subpopulations, NK-L2 (1062 nuclei, 31.0 % of NK-like cells) exhibited a distinct gene expression profile that shared closer affinity with T cells in our global analysis (Supplementary Fig. 5; Supplementary Table 9). However, NK-L2 did not express *cd3*, *tcf7* (ENSSSAG00000006857), *bcl11b* (ENSSSAG00000071984) and *tbx21* (ENSSSAG00000015324), so is unlikely to represent a T cell subpopulation (Supplementary Fig. 5). NK-L2 also expressed distinct cytotoxicity-related factors to NK-L1 and 3NK-L, including genes encoding perforin and granulysin (Supplementary Fig. 5). Additionally, *eomes* (ENSSSAG00000067359), the mammalian T-box transcription factor necessary for late NK cell development and effector functions [136], showed specific expression in NK-L2 and was previously shown to be expressed in rainbow trout NK-like cells [137].

3.2.4. Evidence for macrophages, infiltrating monocytes and dendritic cell subpopulations

Macrophage and monocyte-like cells are long-recognized in salmonids [138] and their responses to *Aeromonas salmonicida* infection have been reported [139]. Further, DC-like cells have been described in salmonid blood [140] and immune organs [141,142]. We identified putative populations of macrophages/monocytes and DCs, along with a distinct MP-L (*cfsr1*-) population (Fig. 4; Supplementary Table 10). The clusters were divided into two major groups: i) macrophages/monocytes (MP1, MP2, MP4, MP6, MP7), based on expression of *marco* (ENSSSAG00000063051) a classic macrophage marker [143] used to identify Atlantic salmon macrophages/monocytes [144] and ii) DC-like (MP3, MP5 and MP-L *csfr1*-) (Fig. 4B and C).

MP1 (2790 nuclei, 49.4 % of MPs) likely represents resident macrophages based on the expression of *prkcdb* (ENSSSAG00000078795) [145], *rxraa* (ENSSSAG00000067352) [146], *lrp1ab* (ENSSSAG00000076721) [147], *marco* [148], *cd4-2.2* (ENSSSAG00000076595) [149] and *timd4* (ENSSSAG00000087400) [149] (Fig. 4C). MP6 (94 nuclei, 1.7 % of MPs) was annotated as resident macrophages undergoing proliferation due to the co-expression of resident macrophage markers and proliferation associated genes (Fig. 4C). MP2 (1145 nuclei, 20.3 % of MPs) likely represents infiltrating macrophages derived from blood monocytes based on upregulation of *cxcr3* (ENSSSAG00000051147) [150], *itgal* (ENSSSAG00000046996) [151], *alox5ap* (ENSSSAG00000006974) [152] and high levels of a *csf1r* paralogue (ENSSSAG00000061479) [60] (Fig. 4C). Although several subtypes of macrophage activation states have been described in teleosts, macrophages are most commonly assigned as either classically activated M1 or alternatively activated M2 macrophages [153]. Adhering to this framework, the blood-borne macrophages/monocytes (MP2) and tissue resident macrophages (MP1) might be considered as M1-like and M2-like, respectively [148,154]. However, the M1/M2 paradigm has become increasingly controversial [155]. In our study, the classical M2 marker gene *cd206* (alias: *mrc1b*) (ENSSSAG00000039787) [156] was upregulated in MP2 (Supplementary Table 10). The Atlantic salmon orthologue of the M2 marker gene *timp2* (ENSSSAG00000100687, ENSSSAG00000091339 and ENSSSAG00000087937) from common carp (*Cyprinus carpio*) [157] was also significantly upregulated in our M1-like population (Supplementary Table 10).

MP4 (313 nuclei, 5.5 % of MPs) potentially represents melanomacrophages based on the expression of resident macrophage markers, alongside strong upregulation of many genes encoding master iron storage and regulating proteins [14], including *frim* (encoding ferritin middle subunit) (ENSSSAG00000010802), *hmox* (ENSSSAG00000039415 and ENSSSAG00000000719), *slc11a2* (ENSSSAG00000081436) and *hmox1a* (ENSSSAG00000070727 and ENSSSAG00000006231) (Fig. 4C; Supplementary Table 10). Melanocytes have long been believed to be derived from the neural crest, arising from the embryonic ectoderm germ layer. Notably, genes involved in the melanogenesis pathway have been shown to be expressed in the spleen [158]. It would significantly alter our understanding of pigmented cells if we could demonstrate that melanomacrophages are capable of synthesizing melanin. However, a range of genes associated with melanin synthesis, namely *mitf*, *mitfa*, *tyr*, *dct* and *sox10*, were not detected in our dataset. The lack of detection of these markers may represent a sensitivity issue and more work is required to investigate the melanin synthesis potential of melanomacrophages.

MP7 (50 nuclei, 0.9 % of MPs) was annotated as 'inflammatory state macrophages/monocytes', due to the large number of specific or highly upregulated marker genes associated with pro-inflammatory functions (Fig. 4C; Supplementary Table 10), including *saa* (ENSSSAG00000100178) [159], *ccl19* (ENSSSAG00000071823) [83], *il8* (ENSSSAG00000006498) [160], *tlr5* (ENSSSAG00000098480) [161] and *camp* (ENSSSAG00000049319) [162,163].

MP3 (158 nuclei, 2.8 % of MPs) showed strong upregulation of *xcr1* (ENSSSAG00000096789) and *cd103* (alias: *itgae*, ENSSSAG00000076346) (Fig. 5A), conserved markers for the mammalian Type 1 conventional dendritic cell subset (cDC1) and avian conventional DCs (cDCs) [164–167]. MP5 (158 nuclei, 2.8 % of MPs) expressed several classic plasmacytoid DCs (pDC) marker genes including *tcf4* (ENSSSAG00000113835, ENSSSAG00000071044), *irf7* (ENSSSAG00000076373) and *cxcr3.1* (ENSSSAG00000115800) [168–170]

(Fig. 5A). However, the mammalian pDC marker *ptprsa* (ENSSSAG00000051752) [171] was highly expressed in MP3. Another mammalian pDC markers *havcr1* (ENSSSAG00000042639) [172], which has been reported in chicken XCR1+ cDCs [173], was also highly expressed in MP3. A gene predicted to encode the transcriptional regulator DC-SCRIPT *zbtb46* (ENSSSAG00000000929), which promotes cDC expression and defines the cDC lineage in mammals [174–176], was highly expressed in both MP3 and MP5 (Fig. 5A). cDC1-like and pDC-like cells have recently been identified in zebrafish [177]. These data suggest that these dendritic cell subsets arose in an early vertebrate ancestor, more than 450 million years ago. Further studies will be required to determine if teleost DC subsets also exhibit functional conservation with their mammalian counterparts.

MP-L (*csfr1*-) expressed many unique marker genes, but lacked markers classically distinguishing cDCs and pDCs (Fig. 5A; Supplementary Table 10). To better understand its global relationship with the other MP clusters, we performed a correlation analysis of the expression levels of all genes for all pairwise combinations of MP cell clusters (Fig. 5B). MP-L (*csfr1*-) showed a higher correlation in marker gene expression with MP3 and MP5 than MP clusters annotated as macrophages/monocytes, supporting a closer global affinity to DCs (Fig. 5B). Further, the extent of transcriptomic correlation between MP- (*csfr1*-) and either MP3 or MP5 was similar to the pairwise comparison between MP3 and MP5 (Fig. 5B). This analysis also validated the close transcriptomic affinity of the identified melanomacrophages (MP4) to resident macrophages (MP1), in addition to a close relationship between infiltrating monocytes (MP2) and the inflammatory state macrophages/monocytes (MP7) (Fig. 5B), indicating the latter are derived from the former.

To provide additional insights into the phenotype of MP-L (*csfr1*-) in relation to the other MP clusters, we performed gene set enrichment analysis separately on each cluster using all significant marker genes (Fig. 5C; Supplementary Table 17). MP-L (*csfr1*-) shared more GO-BP terms in common with MP3 and MP5 than clusters annotated as macrophages/monocytes (Fig. 5C). For example, the term *immune response regulating signalling pathway* was commonly enriched for MP3, MP5 and MP-L (*csfr1*-), but none of the other MP clusters (Fig. 5C). MP-L (*csfr1*-) also shared enriched terms specifically with either MP3 or MP5, but none of the other clusters, including *small GTPase mediated signal transduction* (with MP3) and *phospholipid transport* (with MP5). MP-L (*csfr1*-) also showed several uniquely enriched terms related to the actin cytoskeleton, tyrosine phosphorylation, phagocytosis, and intriguingly, haematopoiesis (*hemopoiesis* and *hematopoietic or lymphoid organ development*) (Fig. 5C). The enrichment of these terms is consistent with a phagocytic, antigen-presenting DC. For example, the actin cytoskeleton is a central component of the immunological synapse formed between DCs and T cells, which is critically regulated by the Rho family of small GTPases [178]. Moreover, tyrosine phosphorylation is elevated locally where T cells-DC synapses form [179]. Among the six marker genes explaining the enriched term *hemopoiesis* was *flt3*, which is expressed in both hematopoietic stem cells and early stage myeloid and lymphoid cells, in addition to mature DCs [70]. Also upregulated was *sh2b3* (ENSSSAG00000071130) a negative regulator of haematopoiesis, encoding an adapter protein that interacts with Jak2 (which was notably a marker for the MP-L *csfr1*-lineage; ENSSSAG00000005849) and regulates actin cytoskeleton development [180]. The enrichment of haematopoiesis genes in this DC subpopulation is interesting and implies these cells are potentially at an earlier stage of development than MP3 and MP5. This might also explain the observation that MP-L *csfr1*-expresses marker genes typically characteristic of diverse immune cells of both the myeloid and lymphoid lineage.

The GO-BP analysis further supported our annotation of MP7 as inflammatory state macrophages/monocytes, for example enriched terms including *defense response to bacterium* (Supplementary Table 17). In addition, MP4 was specifically enriched in terms that are consistent with our annotation of melanomacrophages, including *iron ion transport* and *heme metabolic process*, while MP6 was specifically enriched in cell cycle processes.

3.3. Splenic immune cell responses to aeromonas infection

Past work in salmonids demonstrated that live *Aeromonas* pathogen administered by intraperitoneal injection was localised in multiple immune tissues during the early days of infection, including head kidney, spleen, gill and intestine [181]. Our past liver study using the same animals provided evidence for a strong acute phase response in the *Aeromonas*-infected fish, consistent with the early inflammatory stage of a systemic infection [31]. Consequently, in this study we interpret changes in immune cell composition and expression responses to *Aeromonas* infection assuming the bacteria was localised in the spleen, whilst also infecting other immune tissues.

3.3.1. Limited changes in immune cell composition following infection

We initially asked if changes in splenic cell composition accompanied *Aeromonas* infection. For example, in our past study of liver using the same animals, we observed striking differences in the proportion of infection-associated hepatocyte subpopulations, interpreted to be driving the acute phase response [31]. This approach has the major caveat that we used n = 2 per condition, meaning any observed differences must be interpreted cautiously, pending further validation. With that said, barring the granulocytes, we did not observe strong evidence for infection-associated shifts in the proportion of any major splenic cell type presented in Fig. 1. For the granulocytes, the mean proportion of nuclei was 0.06 for infected fish, compared to 0.03 for control fish, and the individual values within conditions did not overlap across conditions (raw data in Supplementary Table 5). While consistent with the recruitment of granulocytes to the spleen, this difference may have arisen by chance.

We identified candidate changes in the composition of seven immune subpopulations described in Section 3.2, namely B1, B2, T7, T10, T12, MP1 and MP2, where there was no overlap between the proportion of nuclei within a cluster for the two replicates when comparing control and infected conditions (Supplementary Fig. 6; raw data in Supplementary Table 14). The strongest observed difference was for *igt* + B2, where the mean proportion of nuclei comparing infected and control fish (among all B cells) was 0.05 versus 0.14, respectively. This is consistent with *igt* + B2 cells exiting the spleen following infection. Reciprocally, B1, annotated as resting mature B cells, showed a higher mean proportion (among all B cells) of 0.87 in infected fish compared to 0.77 in control fish, which may simply represent a product of the reduced proportion of B2 cells, assuming their exit from the spleen.

MP2, annotated as infiltrating monocytes, showed a higher mean proportion of nuclei (among all MPs) in infected (0.25) than control (0.17) fish, consistent with the recruitment of monocytes to the spleen in response to *Aeromonas* infection. MP1, annotated as resident macrophages, showed a slightly higher mean proportion of nuclei (among all MPs) in the control (0.52) than infected (0.44), which may simply reflect the relative increase in MP2 cells, assuming these are monocytes entering the spleen. T12, annotated as cytotoxic proliferating T cells, showed a higher mean proportion (among all T cells) in infected fish (0.02) than controls (0.01), consistent with increased proliferation of this cell type in response to infection. The potential changes noted for T7 and T10 were small in magnitude.

3.3.2. Differential expression responses

Changes in cellular composition offer only one indicator of the host response to infection, another being differentially expressed genes (DEGs) across cell types. DEG analyses have greater power to detect differences, with statistical power drawn from the large number of cells available. In that respect, it is important to reiterate that all four samples contributed markedly to all identified cell populations (Supplementary Fig. 1; Supplementary Table 5; Supplementary Table 14), meaning the

DEGs were being drawn from two fish per tested condition.

1313 and 1434 genes were upregulated and downregulated, respectively, 24 h post-*Aeromonas* infection across the major spleen cell populations (Fig. 6A; Supplementary Table 15). There was a large variation in response across different cell clusters, with some cell types showing few or zero differentially expressed genes, and others showing a major remodelling of transcriptome (Fig. 6A). The majority of differential expression responses were private to each major cell lineage, with MPs (n = 988), mesenchymal cells (n = 573), B cells (n = 277), and endothelial cells (n = 249) showing the highest number of cell-type specific DEGs (Fig. 6A). Fewer cell-specific DEGs were detected in T cells (n = 78), granulocytes (n = 76) and the NK-L (n = 74) and MP-L *csfr1*- (n = 11) clusters (Fig. 6A). We focussed our effort on interpreting transcriptomic responses to *Aeromonas* using the finer-grained definition of immune cell populations (i.e. Section 3.2), where the number of cell-type specific and shared DEGs again varied strongly across clusters (Fig. 6B; Supplementary Table 16). Only immune subpopulations showing ≥5 cell type-specific DEGs are plotted in Fig. 6B.

3.3.3. *B cell responses to infection*

The B1 subpopulation showed a strong early response to *Aeromonas* infection, with 160 and 139 genes uniquely upregulated or downregulated, respectively (Fig. 6B; Supplementary Table 16). Notably, several transcription factors controlling B cell fate showed significant induction. This included *stat3*, which is required for B lymphopoiesis, GC development, and plasma cell egress from GCs in mammals [182,183] and was one of very few genes altered by *Aeromonas* infection in B cells within Atlantic salmon liver [31]. Also upregulated were *runx1*, and *foxo1*, both encoding transcription factors involved in the regulation of splenic B cell activation and maturation [184,185]. Additionally, B1

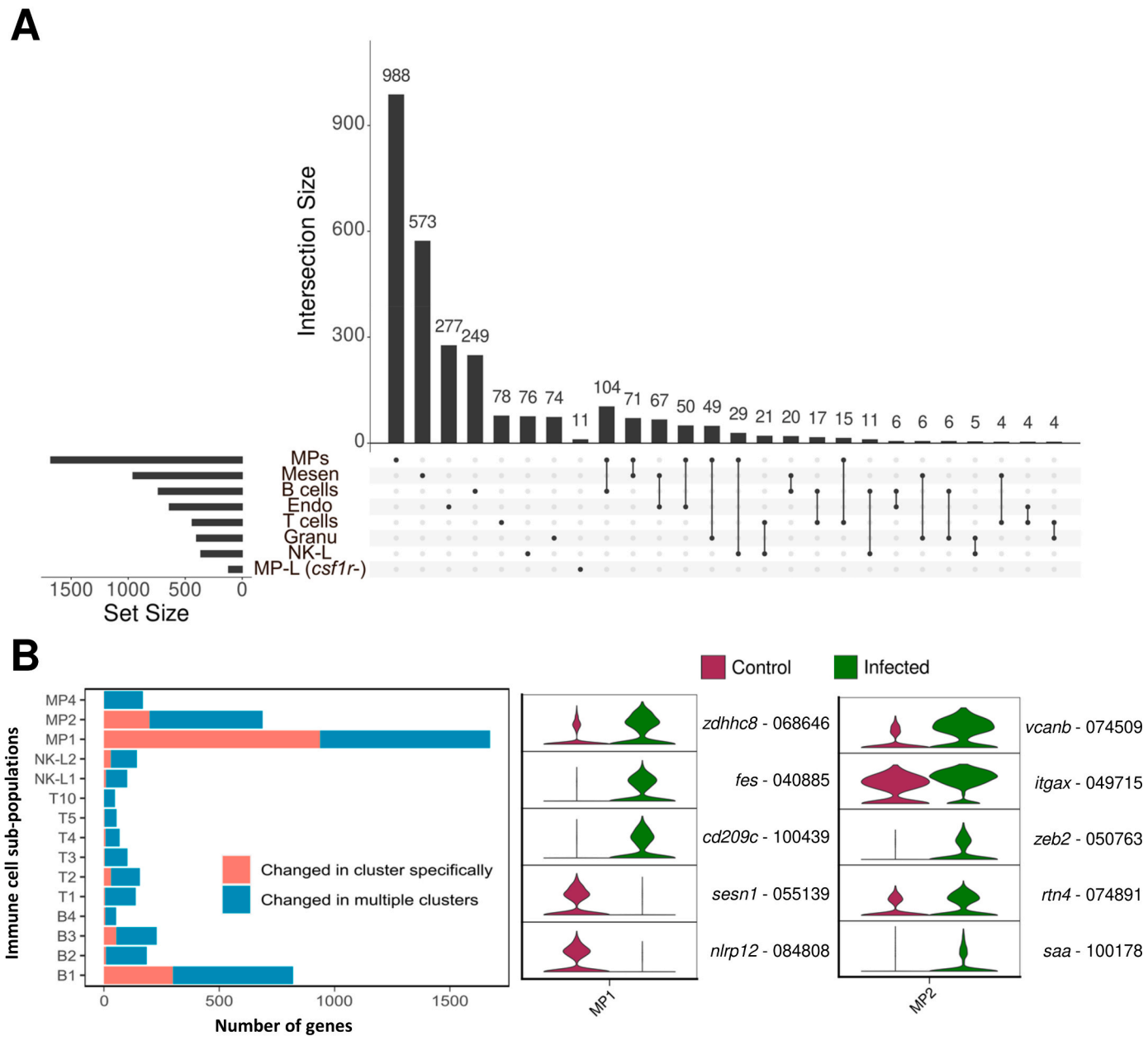

Fig. 6. Differential gene expression across cell populations for control versus *Aeromonas* infected fish. **A**. Upset plot showing genes changed by infection across the major spleen cell lineages. **B**. Numbers of genes altered by *Aeromonas* infection among different immune cell subpopulations. Red and blue bars represent genes changed in single clusters or multiple clusters, respectively. Subpopulations with less than 40 changed genes are not shown. **C.** Violin plots for strongly differentially expressed genes in MP1 and MP2 subpopulations, representing resident macrophages and infiltrating monocytes, respectively.

downregulated *pax5* and *cd63* (ENSSSAG00000043967) [186], indicating a transition towards a more mature B cell phenotype in response to bacterial antigen. We also identified the upregulation of *dock8* (ENSSSAG00000009537) and *fut8* (ENSSSAG00000069930), essential for antigen recognition in mammalian B cells [187,188].

3.3.4. Evidence for homing of immune subpopulations to the gut in response to Aeromonas infection

While the *igt* + B2 subpopulation only showed nine specifically DEGs, a notable non-specific DEG was *ccr9*, with two paralogous copies upregulated (ENSSSAG00000103772; ENSSSAG00000071116). In mammals, *ccr9* encodes a C–C chemokine receptor involved in the homing of activated splenic IgA + B cells to the gut [189]. Considering that teleost IgT is involved in mucosal immunity [190], the upregulation of *ccr9* suggests splenic *igt* + B cells are being primed for gut recruitment upon activation. Further studies would be needed to find out if this upregulation of *ccr9* is a general feature of *igt* + B cell activation that would be stimulated by any activating antigen, or if it is also influenced by the specific pathogen and route of entry. The gut is an entry point for *Aeromonas* in salmonids [191], while intraperitoneal injection of live *Aeromonas* was followed by detection of the bacteria in the salmonid gut during the early stages of infection [181]. The upregulation of *ccr9* in B2 of infected fish is also consistent with the greatly reduced proportion of B2 compared to controls, noted in the last section, assuming these cells are leaving the spleen and homing to gut tissues. The second most upregulated gene in B2 (ENSSSAG00000038144) encodes a protein sharing 93 % identity with an IgT protein annotated by NCBI (accession number: ADD59859), distinct to the *igt* genes previously noted as enriched in B2 (Fig. 2D). Past work has shown that IgT + B cells increase IgT secretion in response to bacterial PAMPs and have innate immune functions including phagocytosis and killing of intracellular bacteria [192].

T2 and T4, annotated as *cd4*+ T helper cells and the single *cd8*+ subpopulation, respectively, also upregulated the same *ccr9* genes (T4: ENSSSAG00000103772 and ENSSSAG00000071116; T2: ENSSSAG00000071116) as B2, similarly suggesting priming for homing to the gut based on mammalian literature [193]. A role for *ccr9* T cell gut homing was previously proposed in European seabass (*Dicentrarchus labrax*) (Galindo-Villegas et al., 2013). *ccr9* (ENSSSAG00000071116) was otherwise only upregulated in MP2, annotated as monocytes. In mammals, *ccr9* upregulation in monocytes is again a signal of recruitment to the gut during inflammation [194].

Overall, the evidence available supports that *igt* + B cells, alongside T cells and monocytes are upregulating *ccr9* to promote homing to the gut to help clear bacteria infiltrating this tissue, representing an interesting hypothesis for further exploration using the marker genes reported in this investigation.

Plasma cell subpopulation B3 specifically upregulated 54 genes including *blimp1/prdm1* (ENSSSAG00000062775), which as noted earlier encodes a master transcription factor for plasma cell differentiation [195]. However, B3 showed downregulation of *irf4b*, another key transcription factor for plasma cell differentiation [97]. Other transcription factor genes showing upregulation in response to *Aeromonas* infection likewise suggest a suppression of plasma cell differentiation, including *foxp1* (ENSSSAG00000077820) and *bcl6aa* (ENSSSAG00000077820), which are both repressors of *prdm1* and *irf4* [196,197].

3.3.5. T cell subpopulation infection responses

Among the 12 T cell populations, T2 (annotated as *cd4*+ T helper cells; Fig. 3) exhibited the strongest response to *Aeromonas* infection with 31 genes showing expression changes specific to this cluster (Fig. 6B; Supplementary Table 16). The top upregulated gene in T2 was *plxnd1* (ENSSSAG00000079145), a gene that negatively regulates differentiation to Th1 cells and promotes differentiation to Th2 and Th17 subsets [198]. The second most regulated gene in T2 was *cd9* (ENSSSAG00000079939), a gene facilitating the interaction between T lymphocytes and antigen-presenting cells [199,200] that stimulates Th2 differentiation [201]. T2 further showed upregulation of *hpgds* (ENSSSAG00000076223), encoding hematopoietic PG D synthase, which is expressed in Th2 cells at sites of antigen presentation in humans [202]. This data suggest that splenic *cd4*+ helper cells acquire a Th2 phenotype upon *Aeromonas* infection. However, it should be noted that *gfi1ab* (ENSSSAG00000038567), a gene encoding a master transcription factor that promotes Th2 differentiation and represses Th1 and Th17 differentiation in mammals [203], was strongly downregulated at the same time. Other T cell subpopulations showed limited changes in response to *Aeromonas* infection.

3.3.6. NK-L cells showed a limited response to Aeromonas infection

NK-L1 and 2NK-L showed cluster-specific differential expression of 9 and 30 genes, respectively (Fig. 6B; Supplementary Table 16). The top upregulated gene in NK-L1 was *gimap7* (ENSSSAG00000088313), encoding a GTPase that showed highest expression in human NK cells according to the human protein atlas [204]. The top upregulated gene in NK-L2 was *prdm16* (ENSSSAG00000063975), which encodes a transcription factor that has not been associated with NK cells in other taxa. NK-L2 also specifically downregulated *ralb* (ENSSSAG00000098007), a key regulator of cytotoxicity in human NK cells [205]. Overall, the signal of differential expression in both NK-L subpopulations was limited.

3.3.7. Macrophages and monocytes showed a strong response to infection

Resident macrophage subpopulation MP1 exhibited the strongest response to *Aeromonas* infection, with 550 and 387 genes specifically upregulated or downregulated, respectively (Fig. 6B; Supplementary Table 16). The top upregulated gene was *zdhhc8* (ENSSSAG00000068646) (Fig. 6C), predicted to encode a palmitoyltransferase, which is likely involved in S-palmitoylation activity, a process with broad roles in shaping macrophage function upon infection [206]. Among the top uniquely upregulated genes in MP1 was *fes* (ENSSSAG00000040885) (Fig. 6C), predicted to encode a cytoplasmic protein tyrosine kinase that reduces survival in mice following LPS challenge [207], and modulates the immune response of resident macrophages to bacterial lipopolysaccharide [208]. Also highly upregulated in MP1 was a gene identified as *cd209c* (ENSSSAG00000100439) (Fig. 6C), a C-type lectin receptor characterised in tongue sole (*Cynoglossus semilaevis*) and shown to bind to and phagocytose different types of bacteria, functions conserved in mammalian macrophages [209]. Among the top uniquely downregulated genes in MP1 was *sesn1* (ENSSSAG00000055139) (Fig. 6C), encoding sestrin1, which was shown to be a negative regulator of inflammasome activation in mammalian macrophages (Keping et al., 2020). Consistent with this interpretation, *nlrp12* (ENSSSAG00000084808), predicted to encode NACHT, LRR and PYD domains-containing protein 12, which is thought to represent a negative regulator of inflammation in mammals [210], was also downregulated (Fig. 6C). The downregulation of *sesn1* and *nlrp12* likely reflects that the *Aeromonas* infection was in the inflammatory phase, consistent with our previous study of the liver using the same fish individuals, where the acute phase response was strongly evident [31].

The infiltrating monocyte cluster MP2 showed cluster-specific differential expression of 198 genes. The top upregulated gene was *vcanb* (ENSSSAG00000074509) (Fig. 6C), encoding versican, which in mammals was strongly upregulated in response to bacterial PAMPs and during the differentiation of monocytes to macrophages, where it likely mediates pro-inflammatory functions [211]. Also upregulated was *itgax* (ENSSSAG00000049715) (alias: CD11c) (Fig. 6C), which is a defining marker for DCs, and thus supports the notion that some infiltrating monocytes may be differentiating into DCs [212]. The upregulation of *zeb2* (ENSSSAG00000050763) (Fig. 6C), a transcription factor required for tissue-specific macrophage identity in spleen and other tissues [213], suggest these monocytes are also becoming inflammatory macrophages following immune stimulation. This is consistent with the upregulation

of *rtn4* (ENSSSAG00000074891) (Fig. 6C), encoding reticulon 4 (alias: Nogo-B), which plays a crucial role in monocyte/macrophage infiltration at sites of inflammation [214]. The specific upregulation of *saa* (ENSSSAG00000100178) in MP2 (Fig. 6C) further suggests these cells were contributing to an inflammatory state following infection.

The candidate DC subpopulations (MP3, MP5 and MP-like (*csfr1*-)) and melanomacrophages (MP4) showed very limited responses to *Aeromonas* infection.

4. Conclusion

Here we successfully deployed snRNA-seq as a cutting-edge technology to identify the major cell types within the Atlantic salmon spleen based on transcriptome-wide information. Considered alongside a 'sister' article investigating cellular heterogeneity within the Atlantic salmon head kidney [33], our study advances understanding of salmonid immunity, while providing useful resources for future work. We provide comprehensive molecular evidence for diverse immune cell lineages and subpopulation phenotypes. The striking variation in response of different splenic cell types and subpopulations to *Aeromonas* infection emphasises the importance of resolving cell-specific expression when monitoring immunological responses. Had this study been performed using bulk transcriptomics, the cell-specific origin of expression would have been masked, and differentially expressed genes specific to less abundant cell types would have been overlooked. Our study also provides a large catalogue of novel marker genes (or validates existing marker genes/paralogues) for different cell types within the Atlantic salmon spleen, which can be leveraged in future studies of the fish immune system. These marker genes can be used to design new antibodies, RNA probes or other molecular reagents targeting different cell types, allowing the spatial organization of the salmonid spleen and other immune sites to be mapped at high resolution. The marker genes generated by this study provide novel targets for genome editing to explore cell-specific functions in the salmonid immune system, and increase scope to prioritize candidate causal genes within quantitative trait loci regions for disease resistance traits [22]. It is of course vital to note the caveat that most of our cell population interpretations rely on existing knowledge derived from studies performed in other species, mainly distantly related mammals. This is a common challenge for single cell studies in non-model fish species, and demands extensive further research - building on knowledge and resources gained via single cell transcriptomics - to deliver a species-specific understanding of cell types and function, including for the Atlantic salmon immune system.

Ethics statement

The Animal work was carried out in compliance with the Animals (Scientific Procedures) Act 1986 under Home Office license PFF8CC5BE and was approved by the ethics committee of the University of Aberdeen.

Funding

This study was funded by grants from the University of Edinburgh's Data Driven Innovation Initiative (Scottish Funding Council Beacon 'Building Back Better' Call) (DJM, RT, RRD) and the Biotechnology and Biological Sciences Research Council, including the Roslin Institute's institutional strategic programme (ISP) awards BBS/E/D/10002071, BBS/E/RL/230001C, BBS/E/D/20002174, BBS/E/RL/230002B, and the responsive mode grants BB/W005859/1 (DJM) and BB/W008564/1 (SAM). AA and JHF were supported by the Research Council of Norway (Project number: 302,191). NH is supported by a Wellcome Trust Senior Research Fellowship in Clinical Science (ref. 219542/Z/19/Z).

CRediT authorship contribution statement

Jianxuan Sun: Methodology, Validation, Investigation, Formal analysis, Visualization, Data curation, Writing – original draft. **Rose Ruiz Daniels:** Conceptualization, Methodology, Validation, Funding acquisition, Writing – review & editing. **Adam Balic:** Supervision, Writing – review & editing. **Adriana M.S. Andresen:** Formal analysis, Writing – review & editing. **Håvard Bjørgen:** Writing – review & editing. **Ross Dobie:** Investigation. **Neil C. Henderson:** Resources, Project administration, Supervision. **Erling Olaf Koppang:** Supervision, Writing – review & editing. **Samuel A.M. Martin:** Resources, Writing – review & editing. **Johanna Hol Fosse:** Supervision, Formal analysis, Writing – review & editing. **Richard S. Taylor:** Conceptualization, Supervision, Funding acquisition, Formal analysis, Data curation, Writing – review & editing. **Daniel J. Macqueen:** Conceptualization, Methodology, Project administration, Visualization, Resources, Funding acquisition, Supervision, Writing – original draft.

Declaration of competing interest

The authors declare that the research was conducted in the absence of any commercial or financial relationships that could be construed as a potential conflict of interest.

Data availability

Data availability statement: All data generated in this study has been made available in the GEO database (https://www.ncbi.nlm.nih.gov/geo/). Accession: GEO accession: GSE252828.

Acknowledgements

We thank Shahmir Naseer for his help during the sampling of fish used in this study.

Appendix A. Supplementary data

Supplementary data to this article can be found online at https://doi.org/10.1016/j.fsi.2024.109358.

References

[1] H.R. Neely, M.F. Flajnik, Emergence and evolution of secondary lymphoid organs, Annu. Rev. Cell Dev. Biol. 32 (2016) 693–711.
[2] R.E. Mebius, G. Kraal, Structure and function of the spleen, Nat. Rev. Immunol. 5 (8) (2005) 606–616.
[3] S.M. Lewis, et al., Structure and function of the immune system in the spleen, Science immunology 4 (33) (2019) eaau6085.
[4] M.F. Cesta, Normal structure, function, and histology of the spleen, Toxicol. Pathol. 34 (5) (2006) 455–465.
[5] A. Brendolan, et al., Development and function of the mammalian spleen, Bioessays 29 (2) (2007) 166–177.
[6] A. Cerutti, et al., Marginal zone B cells: virtues of innate-like antibody-producing lymphocytes, Nat. Rev. Immunol. 13 (2) (2013) 118–132.
[7] H. Matz, H. Dooley, 450 million years in the making: mapping the evolutionary foundations of germinal centers, Front. Immunol. 14 (2023).
[8] L. Mesin, et al., Germinal center B cell dynamics, Immunity 45 (3) (2016) 471–482.
[9] U. Kalan, Flowcytometric Assessment of B Cell Development and Functional Assays on B Cell Development, 2022.
[10] H. Matz, et al., Organized B cell sites in cartilaginous fishes reveal the evolutionary foundation of germinal centers, Cell Rep. 42 (7) (2023).
[11] H. Bjørgen, E.O. Koppang, Anatomy of teleost fish immune structures and organs, Principles of Fish Immunology (2022) 1–30.
[12] C. Agius, R. Roberts, Melano-macrophage centres and their role in fish pathology, J. Fish. Dis. 26 (9) (2003) 499–509.
[13] D. Waly, et al., Immunoglobulin VDJ repertoires reveal hallmarks of germinal centers in unique cell clusters isolated from zebrafish (Danio rerio) lymphoid tissues, Front. Immunol. 13 (2022) 7032.
[14] N.C. Steinel, D.I. Bolnick, Melanomacrophage centers as a histological indicator of immune function in fish and other poikilotherms, Front. Immunol. 8 (2017) 827.

[15] Y. Shibasaki, et al., Cold-blooded vertebrates evolved organized germinal center like structures, Science immunology (0) (2023) eadf1627.
[16] D.A. Jaitin, et al., Massively parallel single-cell RNA-seq for marker-free decomposition of tissues into cell types, Science 343 (6172) (2014) 776–779.
[17] F. Qi, et al., Single cell RNA sequencing of 13 human tissues identify cell types and receptors of human coronaviruses, Biochem. Biophys. Res. Commun. 526 (1) (2020) 135–140.
[18] E. Madissoon, et al., scRNA-seq assessment of the human lung, spleen, and esophagus tissue stability after cold preservation, Genome Biol. 21 (1) (2020) 1–16.
[19] P. Topchyan, et al., Spatial transcriptomics demonstrates the role of CD4 T cells in effector CD8 T cell differentiation during chronic viral infection, Cell Rep. 41 (9) (2022) 111736.
[20] N. Ben-Chetrit, et al., Integration of whole transcriptome spatial profiling with protein markers, Nat. Biotechnol. (2023) 1–6.
[21] J.T. Chan, et al., RNA-seq of single fish cells–seeking out the leukocytes mediating immunity in teleost fishes, Front. Immunol. 13 (2022) 798712.
[22] R. Ruiz Daniels, et al., Single cell genomics as a transformative approach for aquaculture research and innovation, Rev. Aquacult. (2023).
[23] N. Croft Guslund, et al., Lymphocyte subsets in Atlantic cod (Gadus morhua) interrogated by single-cell sequencing, Commun. Biol. 5 (1) (2022) 689.
[24] W. Chen, et al., Multi-tissue scRNA-seq reveals immune cell landscape of turbot (Scophthalmus maximus), Fundamental Research 2 (4) (2022) 550–561.
[25] D. Mu, et al., Single-cell transcriptomic analysis reveals neutrophil as orchestrator during β-glucan–induced trained immunity in a teleost fish, J. Immunol. 209 (4) (2022) 783–795.
[26] F. Asche, T. Bjorndal, The Economics of Salmon Aquaculture, vol. 10, John Wiley & Sons, 2011.
[27] R. Houston, D. Macqueen, Atlantic salmon (Salmo salar L.) genetics in the 21st century: taking leaps forward in aquaculture and biological understanding, Anim. Genet. 50 (1) (2019) 3–14.
[28] D.J. Macqueen, I.A. Johnston, A well-constrained estimate for the timing of the salmonid whole genome duplication reveals major decoupling from species diversification, Proc. Biol. Sci. 281 (1778) (2014) 20132881.
[29] S. Lien, et al., The Atlantic salmon genome provides insights into rediploidization, Nature 533 (7602) (2016) 200–205.
[30] M.K. Gundappa, et al., Genome-wide reconstruction of rediploidization following autopolyploidization across one hundred million years of salmonid evolution, Mol. Biol. Evol. 39 (1) (2022) msab310.
[31] R.S. Taylor, et al., Single cell transcriptomics of Atlantic salmon (Salmo salar L.) liver reveals cellular heterogeneity and immunological responses to challenge by Aeromonas salmonicida, Front. Immunol. (2022) 4755.
[32] A.C. West, et al., Immunologic profiling of the Atlantic salmon gill by single nuclei transcriptomics, Front. Immunol. 12 (2021) 669889.
[33] A.M.S. Andresen, et al., Mapping the cellular landscape of Atlantic salmon head kidney by single cell and single nucleus transcriptomics, Fish Shellfish Immunol. (2024) 109357, https://doi.org/10.1016/j.fsi.2024.109357.
[34] P. Perdiguero, et al., Diversity of rainbow trout blood b cells revealed by single cell RNA sequencing, Biology 10 (6) (2021) 511.
[35] Y. Park, et al., Adherent intestinal cells from Atlantic salmon show phagocytic ability and express macrophage-specific genes, Front. Cell Dev. Biol. 8 (2020) 580848.
[36] R. Ruiz Daniels, et al., A versatile nuclei extraction protocol for single nucleus sequencing in non-model species–Optimization in various Atlantic salmon tissues, Plos one 18 (9) (2023) e0285020.
[37] S. Andrews, FastQC: a quality control tool for high throughput sequence data, in: Babraham Bioinformatics, Babraham Institute, Cambridge, United Kingdom, 2010.
[38] K. Stenløkk, et al., The emergence of supergenes from inversions in Atlantic salmon, Philosophical Transactions of the Royal Society B 377 (1856) (2022) 20210195.
[39] B. Kaminow, et al., STARsolo: accurate, fast and versatile mapping/quantification of single-cell and single-nucleus RNA-seq data, bioRxiv (2021).
[40] Y. Hao, et al., Integrated Analysis of Multimodal Single-Cell Data, Cell, 2021.
[41] M.D. Young, S. Behjati, SoupX removes ambient RNA contamination from droplet-based single-cell RNA sequencing data, GigaScience 9 (12) (2020) giaa151.
[42] C. Hafemeister, R. Satija, Normalization and variance stabilization of single-cell RNA-seq data using regularized negative binomial regression, Genome Biol. 20 (1) (2019) 1–15.
[43] P.-L. Germain, et al., Doublet identification in single-cell sequencing data using scDblFinder, F1000Research 10 (979) (2022) 979.
[44] I. Korsunsky, et al., Fast, sensitive and accurate integration of single-cell data with Harmony, Nat. Methods 16 (12) (2019) 1289–1296.
[45] D. Smedley, et al., The BioMart community portal: an innovative alternative to large, centralized data repositories, Nucleic Acids Res. 43 (W1) (2015) W589–W598.
[46] R. R Core Team, R: A Language and Environment for Statistical Computing, 2013.
[47] G. Yu, et al., clusterProfiler: an R package for comparing biological themes among gene clusters, OMICS A J. Integr. Biol. 16 (5) (2012) 284–287.
[48] T. Stuart, et al., Comprehensive integration of single-cell data, Cell 177 (7) (2019) 1888–1902, e1821.
[49] I. Györy, et al., Transcription factor Ebf1 regulates differentiation stage-specific signaling, proliferation, and survival of B cells, Gene Dev. 26 (7) (2012) 668–682.
[50] M. Peñaranda, et al., Profiling the atlantic salmon IgM+ B cell surface proteome: novel information on teleost fish B cell protein repertoire and identification of potential B cell markers, Front. Immunol. 10 (2019) 37.
[51] B.J. Laidlaw, J.G. Cyster, Transcriptional regulation of memory B cell differentiation, Nat. Rev. Immunol. 21 (4) (2021) 209–220.
[52] G.M. Doody, et al., Signal transduction through Vav-2 participates in humoral immune responses and B cell maturation, Nat. Immunol. 2 (6) (2001) 542–547.
[53] L. Masat, et al., Association of SWAP-70 with the B cell antigen receptor complex, Proc. Natl. Acad. Sci. USA 97 (5) (2000) 2180–2184.
[54] K. Maisey, et al., Identification of CD3ε, CD4, CD8β splice variants of Atlantic salmon, Fish Shellfish Immunol. 31 (6) (2011) 815–822.
[55] S.J. Carmona, et al., Single-cell transcriptome analysis of fish immune cells provides insight into the evolution of vertebrate immune cell types, Genome Res. 27 (3) (2017) 451–461.
[56] P. Kastner, et al., Bcl11b represses a mature T-cell gene expression program in immature CD4+ CD8+ thymocytes, Eur. J. Immunol. 40 (8) (2010) 2143–2154.
[57] J. Lotem, et al., Runx3-mediated transcriptional program in cytotoxic lymphocytes, PLoS One 8 (11) (2013) e80467.
[58] U. Fischer, F. Takizawa, Cellular immune responses, in: Principles of Fish Immunology: from Cells and Molecules to Host Protection, Springer, 2022, pp. 141–176.
[59] E.I. Athanasiadis, et al., Single-cell RNA-sequencing uncovers transcriptional states and fate decisions in haematopoiesis, Nat. Commun. 8 (1) (2017) 2045.
[60] L. Grayfer, et al., Mechanisms of fish macrophage antimicrobial immunity, Front. Immunol. 9 (2018) 1105.
[61] T.T. Tuomisto, et al., Analysis of gene and protein expression during monocyte-macrophage differentiation and cholesterol loading—cDNA and protein array study, Atherosclerosis 180 (2) (2005) 283–291.
[62] M. Chadzinska, et al., Expression profiles of matrix metalloproteinase 9 in teleost fish provide evidence for its active role in initiation and resolution of inflammation, Immunology 125 (4) (2008) 601–610.
[63] J.R. Mathias, et al., Characterization of zebrafish larval inflammatory macrophages, Dev. Comp. Immunol. 33 (11) (2009) 1212–1217.
[64] S. Yamagoe, et al., Purification and primary amino acid sequence of a novel neutrophil chemotactic factor LECT2, Immunol. Lett. 52 (1) (1996) 9–13.
[65] D. Pinheiro, et al., In-silico analysis of myeloid cells across the animal kingdom reveals neutrophil evolution by colony-stimulating factors, Elife 9 (2020) e60214.
[66] A. Rossi, et al., Genetic compensation induced by deleterious mutations but not gene knockdowns, Nature 524 (7564) (2015) 230–233.
[67] J. Bussmann, et al., Zebrafish VEGF receptors: a guideline to nomenclature, PLoS Genet. 4 (5) (2008) e1000064.
[68] D. Welcker, et al., Hemicentin-1 is an essential extracellular matrix component of the dermal–epidermal and myotendinous junctions, Sci. Rep. 11 (1) (2021) 1–16.
[69] S. Brielle, et al., Delineating the heterogeneity of matrix-directed differentiation toward soft and stiff tissue lineages via single-cell profiling, Proc. Natl. Acad. Sci. USA 118 (19) (2021) e2016322118.
[70] H. Karsunky, et al., Flt3 ligand regulates dendritic cell development from Flt3+ lymphoid and myeloid-committed progenitors to Flt3+ dendritic cells in vivo, J. Exp. Med. 198 (2) (2003) 305–313.
[71] J.G. Ogembo, et al., SIRPα/CD172a and FHOD1 are unique markers of littoral cells, a recently evolved major cell population of red pulp of human spleen, J. Immunol. 188 (9) (2012) 4496–4505.
[72] I.R. McCracken, et al., Mapping the developing human cardiac endothelium at single-cell resolution identifies MECOM as a regulator of arteriovenous gene expression, Cardiovasc. Res. 118 (14) (2022) 2960–2972.
[73] Z.-J. Liu, et al., Regulation of Notch1 and Dll4 by vascular endothelial growth factor in arterial endothelial cells: implications for modulating arteriogenesis and angiogenesis, Mol. Cell Biol. 23 (1) (2003) 14–25.
[74] M. Shibuya, Vascular endothelial growth factor receptor-1 (VEGFR-1/Flt-1): a dual regulator for angiogenesis, Angiogenesis 9 (4) (2006) 225–230.
[75] J. Qiu, et al., The characteristics of vessel lining cells in normal spleens and their role in the pathobiology of myelofibrosis, Blood Advances 2 (10) (2018) 1130–1145.
[76] C. Dai, et al., Regulatory mechanisms of Robo4 and their effects on angiogenesis, Biosci. Rep. 39 (7) (2019) BSR20190513.
[77] D. Nichol, H. Stuhlmann, EGFL7: a unique angiogenic signaling factor in vascular development and disease 119 (6) (2012) 1345–1352.
[78] L.A. Strickland, et al., Plasmalemmal vesicle-associated protein (PLVAP) is expressed by tumour endothelium and is upregulated by vascular endothelial growth factor-A (VEGF), J. Pathol.: A Journal of the Pathological Society of Great Britain and Ireland 206 (4) (2005) 466–475.
[79] L. Denzer, et al., The role of PLVAP in endothelial cells, Cell Tissue Res. (2023) 1–20.
[80] M. Pack, et al., DEC-205/CD205+ dendritic cells are abundant in the white pulp of the human spleen, including the border region between the red and white pulp, Immunology 123 (3) (2008) 438–446.
[81] J.M. Cook-Mills, VCAM-1 signals during lymphocyte migration: role of reactive oxygen species, Mol. Immunol. 39 (9) (2002) 499–508.
[82] S. Cambier, et al., The chemokines CXCL8 and CXCL12: molecular and functional properties, role in disease and efforts towards pharmacological intervention, Cell. Mol. Immunol. 20 (3) (2023) 217–251.
[83] I. Comerford, et al., A myriad of functions and complex regulation of the CCR7/CCL19/CCL21 chemokine axis in the adaptive immune system, Cytokine Growth Factor Rev. 24 (3) (2013) 269–283.

[84] P. Zwollo, et al., B cell signatures of BCWD-resistant and susceptible lines of rainbow trout: a shift towards more EBF-expressing progenitors and fewer mature B cells in resistant animals, Dev. Comp. Immunol. 48 (1) (2015) 1–12.
[85] M. Barr, et al., Defining terminally differentiating B cell populations in rainbow trout immune tissues using the transcription factor XbpI, Fish Shellfish Immunol. 31 (6) (2011) 727–735.
[86] P. Zwollo, et al., Molecular and cellular analysis of B-cell populations in the rainbow trout using Pax5 and immunoglobulin markers, Dev. Comp. Immunol. 32 (12) (2008) 1482–1496.
[87] P. Zwollo, et al., B cell heterogeneity in the teleost kidney: evidence for a maturation gradient from anterior to posterior kidney, J. Immunol. 174 (11) (2005) 6608–6616.
[88] J. Ye, et al., Plasmablasts and plasma cells: reconsidering teleost immune system organization, Dev. Comp. Immunol. 35 (12) (2011) 1273–1281.
[89] C. Tsui, et al., Protein kinase C-β dictates B cell fate by regulating mitochondrial remodeling, metabolic reprogramming, and heme biosynthesis, Immunity 48 (6) (2018) 1144–1159, e1145.
[90] M.A. Inlay, et al., Ly6d marks the earliest stage of B-cell specification and identifies the branchpoint between B-cell and T-cell development, Gene Dev. 23 (20) (2009) 2376–2381.
[91] L.M. Ganley-Leal, et al., Toll-like receptor 2-mediated human B cell differentiation, Clin. Immunol. 120 (3) (2006) 272–284.
[92] W.-J. Won, J.F. Kearney, CD9 is a unique marker for marginal zone B cells, B1 cells, and plasma cells in mice, J. Immunol. 168 (11) (2002) 5605–5611.
[93] Q. Zhang, et al., Structures and biological functions of IL-31 and IL-31 receptors, Cytokine Growth Factor Rev. 19 (5–6) (2008) 347–356.
[94] K. Singh, et al., The L-arginine transporter solute carrier family 7 member 2 mediates the immunopathogenesis of attaching and effacing bacteria, PLoS Pathog. 12 (10) (2016) e1005984.
[95] R.L. Gavin, et al., Tspan18 is a novel regulator of thrombo-inflammation, Med. Microbiol. Immunol. 209 (2020) 553–564.
[96] M. Al-Maskari, et al., Site-1 protease function is essential for the generation of antibody secreting cells and reprogramming for secretory activity, Sci. Rep. 8 (1) (2018) 14338.
[97] U. Klein, et al., Transcription factor IRF4 controls plasma cell differentiation and class-switch recombination, Nat. Immunol. 7 (7) (2006) 773–782.
[98] P. Zwollo, Dissecting teleost B cell differentiation using transcription factors, Dev. Comp. Immunol. 35 (9) (2011) 898–905.
[99] M. Minnich, et al., Multifunctional role of the transcription factor Blimp-1 in coordinating plasma cell differentiation, Nat. Immunol. 17 (3) (2016) 331–343.
[100] E. Morel, et al., Endoplasmic reticulum expansion throughout the differentiation of teleost B cells to plasmablasts, iScience 26 (1) (2023) 105854.
[101] F. Stadlbauer, et al., DNA replication in vitro by recombinant DNA-polymerase-α-primase, Eur. J. Biochem. 222 (3) (1994) 781–793.
[102] P. Starokadomskyy, et al., DNA polymerase-α regulates the activation of type I interferons through cytosolic RNA: DNA synthesis, Nat. Immunol. 17 (5) (2016) 495–504.
[103] J. Gerdes, et al., Production of a mouse monoclonal antibody reactive with a human nuclear antigen associated with cell proliferation, Int. J. Cancer 31 (1) (1983) 13–20.
[104] H. Liao, et al., Mitotic regulation of microtubule cross-linking activity of CENP-E kinetochore protein, Science 265 (5170) (1994) 394–398.
[105] C.M. Field, B.M. Alberts, Anillin, a contractile ring protein that cycles from the nucleus to the cell cortex, J. Cell Biol. 131 (1) (1995) 165–178.
[106] Z. Jing, et al., NCAPD3 promotes prostate cancer progression by up-regulating EZH2 and MALAT1 through STAT3 and E2F1, Cell. Signal. 92 (2022) 110265.
[107] P.M. Watt, I.D. Hickson, Structure and function of type II DNA topoisomerases, Biochem. J. 303 (Pt 3) (1994) 681.
[108] F. Wan, et al., Characterization of γδ T cells from zebrafish provides insights into their important role in adaptive humoral immunity, Front. Immunol. 7 (2017) 675.
[109] H.-f. Tian, et al., Cluster of differentiation antigens: essential roles in the identification of teleost fish T lymphocytes, Marine Life Science & Technology 4 (3) (2022) 303–316.
[110] R. Yazawa, et al., Functional adaptive diversity of the Atlantic salmon T-cell receptor gamma locus, Mol. Immunol. 45 (8) (2008) 2150–2157.
[111] J.H. Esensten, et al., CD28 costimulation: from mechanism to therapy, Immunity 44 (5) (2016) 973–988.
[112] F. Takizawa, et al., Novel teleost CD4-bearing cell populations provide insights into the evolutionary origins and primordial roles of CD4+ lymphocytes and CD4 + macrophages, J. Immunol. 196 (11) (2016) 4522–4535.
[113] M.K. Liszewski, et al., Intracellular complement activation sustains T cell homeostasis and mediates effector differentiation, Immunity 39 (6) (2013) 1143–1157.
[114] M. von Essen, et al., Protein kinase C (PKC) α and PKCθ are the major PKC isotypes involved in TCR down-regulation, J. Immunol. 176 (12) (2006) 7502–7510.
[115] M.P. Holt, et al., TCR signaling and CD28/CTLA-4 signaling cooperatively modulate T regulatory cell homeostasis, J. Immunol. 198 (4) (2017) 1503–1511.
[116] A.S. Gokhale, et al., Selective deletion of Eos (Ikzf4) in T-regulatory cells leads to loss of suppressive function and development of systemic autoimmunity, J. Autoimmun. 105 (2019) 102300.
[117] M.A. Gavin, et al., Foxp3-dependent programme of regulatory T-cell differentiation, Nature 445 (7129) (2007) 771–775.
[118] A.Y. Rudensky, Regulatory T cells and Foxp3, Immunol. Rev. 241 (1) (2011) 260–268.
[119] A. Corthay, How do regulatory T cells work? Scand. J. Immunol. 70 (4) (2009) 326–336.
[120] D.J. Topham, E.C. Reilly, Tissue-resident memory CD8+ T cells: from phenotype to function, Front. Immunol. 9 (2018) 515.
[121] G.B. Gmyrek, et al., Polarity gene discs large homolog 1 regulates the generation of memory T cells, Eur. J. Immunol. 43 (5) (2013) 1185–1194.
[122] F. Takizawa, et al., The expression of CD8α discriminates distinct T cell subsets in teleost fish, Dev. Comp. Immunol. 35 (7) (2011) 752–763.
[123] J.T. White, et al., Antigen-inexperienced memory CD8+ T cells: where they come from and why we need them, Nat. Rev. Immunol. 17 (6) (2017) 391–400.
[124] C.T. Herzig, et al., Evolution of the CD163 family and its relationship to the bovine gamma delta T cell co-receptor WC1, BMC Evol. Biol. 10 (2010) 1–19.
[125] M. Lawand, et al., Key features of gamma-delta T-cell subsets in human diseases and their immunotherapeutic implications, Front. Immunol. 8 (2017) 761.
[126] H.J. Melichar, et al., Regulation of γδ versus αß T lymphocyte differentiation by the transcription factor SOX13, Science 315 (5809) (2007) 230–233.
[127] J.M. Heather, et al., Regulation of gammadelta versus alphabeta T lymphocyte differentiation by the transcription factor SOX13, Science 315 (5809) (2007) 5230–5803, https://doi.org/10.1126/science.1135344.
[128] I. Ho, et al., Human GATA-3: a lineage-restricted transcription factor that regulates the expression of the T cell receptor alpha gene, EMBO J. 10 (5) (1991) 1187–1192.
[129] S.K. Nandakumar, et al., Low-level GATA2 overexpression promotes myeloid progenitor self-renewal and blocks lymphoid differentiation in mice, Exp. Hematol. 43 (7) (2015) 565–577, e510.
[130] D. Bending, et al., A timer for analyzing temporally dynamic changes in transcription during differentiation in vivo, JCB (J. Cell Biol.) 217 (8) (2018) 2931–2950.
[131] X. Wang, et al., Reinvestigation of classic T cell subsets and identification of novel cell subpopulations by single-cell rna sequencing, J. Immunol. 208 (2) (2022) 396–406.
[132] U. Fischer, et al., Teleost T and NK cell immunity, Fish Shellfish Immunol. 35 (2) (2013) 197–206.
[133] L. Shen, et al., Channel catfish cytotoxic cells: a mini-review, Dev. Comp. Immunol. 26 (2) (2002) 141–149.
[134] A. Awasthi, et al., Deletion of PI3K-p85α gene impairs lineage commitment, terminal maturation, cytokine generation and cytotoxicity of NK cells, Gene Immun. 9 (6) (2008) 522–535.
[135] M.J. Van Helden, et al., Terminal NK cell maturation is controlled by concerted actions of T-bet and Zeb2 and is essential for melanoma rejection, J. Exp. Med. 212 (12) (2015) 2015–2025.
[136] S.M. Gordon, et al., The transcription factors T-bet and Eomes control key checkpoints of natural killer cell maturation, Immunity 36 (1) (2012) 55–67.
[137] F. Takizawa, et al., Transcription analysis of two Eomesodermin genes in lymphocyte subsets of two teleost species, Fish Shellfish Immunol. 36 (1) (2014) 215–222.
[138] R. Braun-Nesje, et al., Salmonid macrophages: separation, in vitro culture and characterization, J. Fish. Dis. 4 (2) (1981) 141–151.
[139] K.V. Ewart, et al., The early response of Atlantic salmon (Salmo salar) macrophages exposed in vitro to Aeromonas salmonicida cultured in broth and in fish, Dev. Comp. Immunol. 32 (4) (2008) 380–390.
[140] G.T. Haugland, et al., Characterization of small, mononuclear blood cells from salmon having high phagocytic capacity and ability to differentiate into dendritic like cells, PLoS One 7 (11) (2012) e49260.
[141] J. Lovy, et al., Comparative cellular morphology suggesting the existence of resident dendritic cells within immune organs of salmonids, Anat. Rec.: Advances in Integrative Anatomy and Evolutionary Biology: Advances in Integrative Anatomy and Evolutionary Biology 291 (4) (2008) 456–462.
[142] E. Bassity, T.G. Clark, Functional identification of dendritic cells in the teleost model, rainbow trout (Oncorhynchus mykiss), PLoS One 7 (3) (2012) e33196.
[143] G. Kraal, et al., The macrophage receptor MARCO, Microb. Infect. 2 (3) (2000) 313–316.
[144] N.C. Smith, et al., Transcriptome profiling of Atlantic salmon adherent head kidney leukocytes reveals that macrophages are selectively enriched during culture, Front. Immunol. 12 (2021) 709910.
[145] N. Duquesnes, et al., PKC-delta and PKC-epsilon: foes of the same family or strangers? J. Mol. Cell. Cardiol. 51 (5) (2011) 665–673.
[146] J. Philpott, et al., RXRα regulates the development of resident tissue macrophages, ImmunoHorizons 6 (6) (2022) 366–372.
[147] P. May, et al., Low density receptor-related protein 1 (LRP1) promotes anti-inflammatory phenotype in murine macrophages, Cell Tissue Res. 354 (3) (2013) 887–889.
[148] L.C. Davies, et al., Tissue-resident macrophages, Nat. Immunol. 14 (10) (2013) 986–995.
[149] T.N. Shaw, et al., Tissue-resident macrophages in the intestine are long lived and defined by Tim-4 and CD4 expression, J. Exp. Med. 215 (6) (2018) 1507–1518.
[150] X.-J. Lu, et al., CXCR3. 1 and CXCR3. 2 differentially contribute to macrophage polarization in teleost fish, J. Immunol. 198 (12) (2017) 4692–4706.
[151] A.K. Shukla, et al., CD11a expression distinguishes infiltrating myeloid cells from plaque-associated microglia in Alzheimer's disease, Glia 67 (5) (2019) 844–856.
[152] O. Werz, et al., Human macrophages differentially produce specific resolvin or leukotriene signals that depend on bacterial pathogenicity, Nat. Commun. 9 (1) (2018) 59.
[153] M. Forlenza, et al., Heterogeneity of macrophage activation in fish, Dev. Comp. Immunol. 35 (12) (2011) 1246–1255.

[154] A. Mantovani, et al., Macrophage polarization comes of age, Immunity 23 (4) (2005) 344–346.
[155] M. Nahrendorf, F.K. Swirski, Abandoning M1/M2 for a network model of macrophage function, Circ. Res. 119 (3) (2016) 414–417.
[156] M. Orecchioni, et al., Macrophage polarization: different gene signatures in M1 (LPS+) vs. classically and M2 (LPS–) vs. alternatively activated macrophages, Front. Immunol. 10 (2019) 1084.
[157] A.S. Wentzel, et al., Transcriptome sequencing supports a conservation of macrophage polarization in fish, Sci. Rep. 10 (1) (2020) 1–15.
[158] J. Thorsen, et al., Isolation of the Atlantic salmon tyrosinase gene family reveals heterogenous transcripts in a leukocyte cell line, Pigm. Cell Res. 19 (4) (2006) 327–336.
[159] F. Villarroel, et al., Serum amyloid A: a typical acute-phase reactant in rainbow trout? Dev. Comp. Immunol. 32 (10) (2008) 1160–1169.
[160] S.H. Oehlers, et al., Expression of zebrafish cxcl8 (interleukin-8) and its receptors during development and in response to immune stimulation, Dev. Comp. Immunol. 34 (3) (2010) 352–359.
[161] S. Tsoi, et al., Identification of a transcript encoding a soluble form of toll-like receptor 5 (TLR5) in Atlantic salmon during Aeromonas salmonicida infection, Vet. Immunol. Immunopathol. 109 (1–2) (2006) 183–187.
[162] G.M. Kammer, The adenylate cyclase-cAMP-protein kinase A pathway and regulation of the immune response, Immunol. today 9 (7–8) (1988) 222–229.
[163] C.-I. Chang, et al., Two cathelicidin genes are present in both rainbow trout (Oncorhynchus mykiss) and atlantic salmon (Salmo salar), Antimicrob. Agents Chemother. 50 (1) (2006) 185–195.
[164] K. Crozat, et al., The XC chemokine receptor 1 is a conserved selective marker of mammalian cells homologous to mouse CD8α+ dendritic cells, J. Exp. Med. 207 (6) (2010) 1283–1292.
[165] A. Bachem, et al., Expression of XCR1 characterizes the Batf3-dependent lineage of dendritic cells capable of antigen cross-presentation, Front. Immunol. 3 (2012) 214.
[166] J.-Y. Shin, et al., A recently described type 2 conventional dendritic cell (cDC2) subset mediates inflammation, Cell. Mol. Immunol. 17 (12) (2020) 1215–1217.
[167] Z. Wu, et al., Development of novel reagents to chicken FLT3, XCR1 and CSF2R for the identification and characterization of avian conventional dendritic cells, Immunology 165 (2) (2022) 171–194.
[168] M. Kerkmann, et al., Activation with CpG-A and CpG-B oligonucleotides reveals two distinct regulatory pathways of type I IFN synthesis in human plasmacytoid dendritic cells, J. Immunol. 170 (9) (2003) 4465–4474.
[169] B. Vanbervliet, et al., The inducible CXCR3 ligands control plasmacytoid dendritic cell responsiveness to the constitutive chemokine stromal cell–derived factor 1 (SDF-1)/CXCL12, J. Exp. Med. 198 (5) (2003) 823–830.
[170] B. Cisse, et al., Transcription factor E2-2 is an essential and specific regulator of plasmacytoid dendritic cell development, Cell 135 (1) (2008) 37–48.
[171] B. Reizis, Plasmacytoid dendritic cells: development, regulation, and function, Immunity 50 (1) (2019) 37–50.
[172] M. Swiecki, M. Colonna, The multifaceted biology of plasmacytoid dendritic cells, Nat. Rev. Immunol. 15 (8) (2015) 471–485.
[173] Z. Wu, et al., Development and function of chicken XCR1+ conventional dendritic cells, Front. Immunol. 14 (2023) 1–25.
[174] M. Chopin, et al., Transcription factor PU. 1 promotes conventional dendritic cell identity and function via induction of transcriptional regulator DC-SCRIPT, Immunity 50 (1) (2019) 77–90, e75.
[175] E. Zoccola, et al., Identification of barramundi (Lates calcarifer) DC-SCRIPT, a specific molecular marker for dendritic cells in fish, PLoS One 10 (7) (2015) e0132687.
[176] A.T. Satpathy, et al., Zbtb46 expression distinguishes classical dendritic cells and their committed progenitors from other immune lineages, J. Exp. Med. 209 (6) (2012) 1135–1152.
[177] Q. Zhou, et al., Cross-organ single-cell transcriptome profiling reveals macrophage and dendritic cell heterogeneity in zebrafish, Cell Rep. 42 (7) (2023).
[178] J.L. Rodríguez-Fernández, O. Criado-García, The actin cytoskeleton at the immunological synapse of dendritic cells, Front. Cell Dev. Biol. 9 (2021) 679500.
[179] P. Revy, et al., Functional antigen-independent synapses formed between T cells and dendritic cells, Nat. Immunol. 2 (10) (2001) 925–931.
[180] J. Devallière, B. Charreau, The adaptor Lnk (SH2B3): an emerging regulator in vascular cells and a link between immune and inflammatory signaling, Biochem. Pharmacol. 82 (10) (2011) 1391–1402.
[181] M. Tatner, et al., The tissue localization of Aeromonas salmonicida in rainbow trout, Salmo gairdneri Richardson, following three methods of administration, J. Fish. Biol. 25 (1) (1984) 95–108.
[182] W.-C. Chou, et al., STAT3 positively regulates an early step in B-cell development, Blood 108 (9) (2006) 3005–3011.
[183] A.J. Fike, et al., STAT3 signaling in B cells controls germinal center zone organization and recycling, Cell Rep. 42 (5) (2023).
[184] J. Chen, et al., Foxo1 regulates marginal zone B-cell development, Eur. J. Immunol. 40 (7) (2010) 1890–1896.
[185] I. Thomsen, et al., RUNX1 regulates a transcription program that affects the dynamics of cell cycle entry of naive resting B cells, J. Immunol. 207 (12) (2021) 2976–2991.
[186] N. Yoshida, et al., CXCR4 expression on activated B cells is downregulated by CD63 and IL-21, J. Immunol. 186 (5) (2011) 2800–2808.
[187] K.L. Randall, et al., Dock8 mutations cripple B cell immunological synapses, germinal centers and long-lived antibody production, Nat. Immunol. 10 (12) (2009) 1283–1291.
[188] W. Li, et al., Core fucosylation of IgG B cell receptor is required for antigen recognition and antibody production, J. Immunol. 194 (6) (2015) 2596–2606.
[189] D. Weiberg, et al., Participation of the spleen in the IgA immune response in the gut, PLoS One 13 (10) (2018) e0205247.
[190] Y.-A. Zhang, et al., IgT, a primitive immunoglobulin class specialized in mucosal immunity, Nat. Immunol. 11 (9) (2010) 827–835.
[191] E. Ringø, et al., Damaging effect of the fish pathogen Aeromonas salmonicida ssp. salmonicida on intestinal enterocytes of Atlantic salmon (Salmo salar L.), Cell Tissue Res. 318 (2004) 305–311.
[192] Y.-A. Zhang, et al., Recent findings on the structure and function of teleost IgT, Fish Shellfish Immunol. 31 (5) (2011) 627–634.
[193] S. Uehara, et al., A role for CCR9 in T lymphocyte development and migration, J. Immunol. 168 (6) (2002) 2811–2819.
[194] L. Linton, et al., HLA-DR(hi) and CCR9 define a pro-inflammatory monocyte subset in IBD, Clin. Transl. Gastroenterol. 3 (12) (2012) e29.
[195] A. Shaffer, et al., Blimp-1 orchestrates plasma cell differentiation by extinguishing the mature B cell gene expression program, Immunity 17 (1) (2002) 51–62.
[196] J. Alinikula, et al., Alternate pathways for Bcl6-mediated regulation of B cell to plasma cell differentiation, European jocnal of immunology 41 (8) (2011) 2404–2413.
[197] M. Van Keimpema, et al., The forkhead transcription factor FOXP1 represses human plasma cell differentiation 126 (18) (2015) 2098–2109.
[198] T. Carvalheiro, et al., Semaphorin4A-plexin D1 axis induces Th2 and Th17 while represses Th1 skewing in an autocrine manner, Int. J. Mol. Sci. 21 (18) (2020) 6965.
[199] H. Kobayashi, et al., The tetraspanin CD9 is preferentially expressed on the human CD4+ CD45RA+ naive T cell population and is involved in T cell activation, Clin. Exp. Immunol. 137 (1) (2004) 101–108.
[200] V. Rocha-Perugini, et al., Tetraspanins CD9 and CD151 at the immune synapse support T-cell integrin signaling, Eur. J. Immunol. 44 (7) (2014) 1967–1975.
[201] C. Brosseau, et al., CD9 tetraspanin: a new pathway for the regulation of inflammation? Front. Immunol. 9 (2018) 2316.
[202] K. Tanaka, et al., Cutting edge: differential production of prostaglandin D2 by human helper T cell subsets, J. Immunol. 164 (5) (2000) 2277–2280.
[203] J. Suzuki, et al., Gfi1, a transcriptional repressor, inhibits the induction of the T helper type 1 programme in activated CD 4 T cells, Immunology 147 (4) (2016) 476–487.
[204] M. Karlsson, et al., A single–cell type transcriptomics map of human tissues, Sci. Adv. 7 (31) (2021) eabh2169.
[205] J. Sánchez-Ruiz, et al., Ral GTPases regulate cell-mediated cytotoxicity in NK cells, J. Immunol. 187 (5) (2011) 2433–2441.
[206] J. Guns, et al., Protein lipidation by palmitate controls macrophage function, Cells 11 (3) (2022) 565.
[207] R.A. Zirngibl, et al., Enhanced endotoxin sensitivity in fps/fes-null mice with minimal defects in hematopoietic homeostasis, Mol. Cell Biol. 22 (8) (2002) 2472–2486.
[208] S.A. Parsons, P.A. Greer, The Fps/Fes kinase regulates the inflammatory response to endotoxin through down-regulation of TLR4, NF-κB activation, and TNF-α secretion in macrophages, J. Leukoc. Biol. 80 (6) (2006) 1522–1528.
[209] S. Jiang, L. Sun, Tongue sole CD209: a pattern-recognition receptor that binds a broad range of microbes and promotes phagocytosis, Int. J. Mol. Sci. 18 (9) (2017) 1848.
[210] S. Tuladhar, T.-D. Kanneganti, NLRP12 in innate immunity and inflammation, Mol. Aspect. Med. 76 (2020) 100887.
[211] T.N. Wight, et al., Versican and the control of inflammation, Matrix Biol. 35 (2014) 152–161.
[212] C. Ardavín, et al., Origin and differentiation of dendritic cells, Trends Immunol. 22 (12) (2001) 691–700.
[213] C.L. Scott, et al., The transcription factor ZEB2 is required to maintain the tissue-specific identities of macrophages, Immunity 49 (2) (2018) 312–325, e315.
[214] J. Yu, et al., Reticulon 4B (Nogo-B) is necessary for macrophage infiltration and tissue repair, Proc. Natl. Acad. Sci. USA 106 (41) (2009) 17511–17516.